Chapter 4

Oxidation Behavior of Orthorhombic Ti_2AlNb Alloy

Joanna Małecka

Additional information is available at the end of the chapter

http://dx.doi.org/10.5772/63998

Abstract

The results of investigation on the oxidation behavior of orthorhombic Ti_2AlNb alloy with Al_2O_3 and AlCrN coating are presented. Oxidation was carried out in static air atmosphere at 700 and 800°C and in 9% O_2+0.2% HCl+0.08% SO_2+N_2 atmosphere at a temperature of 700–750°C. Investigation of the material structure of the specimen and chemical composition of oxidation products was performed. The surfaces were characterized using SEM (scanning electron microscopy) techniques. It was determined that the alloy shows a sufficient high-temperature corrosion resistance only at 700°C. At both temperatures, the coated samples exhibited reduced mass gain compared to uncoated alloy. At 700°C rather insignificant differences were observed; however, at the temperature of 800°C, the deposited coatings strongly limit the mass gain of the test material.

Keywords: orthorhombic alloys, SEM, high temperature corrosion, oxidation, coatings

1. Introduction

1960s of the twentieth century mark the increased development of research on the mechanisms and kinetics of oxidation of metals and alloys. The theoretical generalizations presented back then provided a lot of valuable information that is relevant today and are of great importance for further development of the theory of corrosion. In principle, every solid undergoes corrosion processes in various degrees, and with the progress of technical development, a number of problems arose in the use of metallic materials at high temperature and their resistance to oxidation. A complete removal of corrosion damage during the construction of materials is not possible; however, the amount of losses can be limited by the selection of suitable material. The observed trend in recent years is the increasing use of materials characterized by

very attractive performance properties, and intermetallic phase TiAl alloys perfectly fit this trend.

The fundamentals behind industrial fabrication of titanium and its alloys are their unique physical and mechanical properties as compared with other construction materials. However, the development of technology creates the need to raise the requirements for engineering materials while ensuring competitiveness at the global level including all industries and is inextricably linked with the need to use materials that are characterized by improved mechanical properties, lower density, and greater resistance to high temperatures.

In recent years, a new group of advanced engineering materials has been formulated, featuring good practical properties, such as greater resistance to high-temperature oxidation in comparison to conventional titanium alloys [1–3], namely titanium alloys based on intermetallic phases. This group of materials, which was researched in the 1950s of the twentieth century, included alloys based on $Ti_3Al(\alpha_2)$ phase, alloys based on $TiAl(\gamma)$ and those based on $TiAl_3$ [3] which show high brittleness. The stimulus for research was the need to produce light and rugged materials for aviation and space industry, and they were supposed to replace titanium alloys and nickel-based alloys used in the construction of jet engines [2,4]. However, titanium alloys based on $TiAl(\gamma)$ have been used as construction materials. They are used in modern plane engines, featuring better efficiency, power saving and lesser emission of exhaust fumes. It should be underlined that new concepts of the development of intermetallics-based titanium alloys are continuously created. Toward the end of the 1980s of the twentieth century, a molecule of $Ti_2AlNb(O)$ [5–9] was introduced into the phase composition of titanium alloys, which caused a rise in their density, but at the same time improved other properties—among others—its plasticity. These materials are still at the research stage and are not yet produced commercially; however, it seems that wide application prospects are open for them and they may become an interesting offer for the modern industry as an alternative for the materials currently in use.

Great research effort [10–14] is put into improving their technological properties, increasing their ductility and resistance to oxidation, which is still the main obstacle for their application, especially in elements designed to have a working life. Alloy heat resistance depends primarily on the protective properties of the scale that forms during the course of oxidation. However, under high temperature, the formed scale is insufficient protection for the substrate material, resulting in its complete or partial destruction within a short period of time. The extension of lifetime of the material can be achieved by coating its surface with a special layer of protective nature. The coating and the substrate protected by it must be treated as a whole in operating conditions; therefore, the selection of the coating material should incorporate a number of specific requirements, and the primary factor should be the rate of diffusion exchange that occurs at high temperatures between the substrate material and the coating [15]. In order to meet the protective role and to be stable, the deposited coating must have properties compatible with the substrate material. Most importantly, these materials must have similar coefficients of thermal expansion to prevent cracking and peeling of the coating during temperature changes. In most cases, good protection of the material is desired for a long time, but in some

http://dx.doi.org/10.5772/63998

cases operating time of the element is limited by other parameters as it is, for example in rocket engines, etc.

It should be noted that not only temperature but also the chemical composition of the corrosive environment has a great impact on oxidation rate. Structural elements working in high temperatures are often subjected not only to hot air action but, first and foremost, to aggressive environment containing sulfur compounds. Current research results show that even little quantities of sulfur compounds lead to a considerable, almost catastrophic increase in the rate of oxidation of titanium alloys based on intermetallic phases, and the resistance of titanium alloys to this type of corrosion is still insufficient.

2. Experimental procedures

The tests were performed on $Ti_2AlNb(O)$-based alloy. The chemical composition of the analyzed material is shown in **Table 1**.

Material	**% at**				
	Al	**Nb**	**Mo**	**V**	**Ti**
$Ti_2AlNb(O)$	25	12.5	6.01	0.48	balance

Table 1. Chemical composition of the material.

Two protective coatings were generated on the surface of the test material:

- Al_2O_3 deposited by sol-gel method,
- AlCrN deposited by physical vapor deposition.

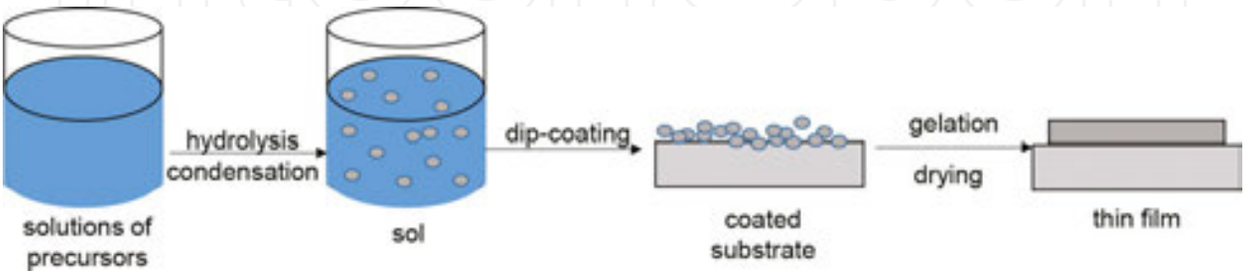

Figure 1. Stages of the dip-coating process.

The sol-gel technology is a gradual process of synthesizing ceramics, glasses or composites, which consists of preparing the sol (solution), formation of sol-gel and removing the solvent [16]. The stages of the process are presented in **Figure 1**. The first step of sol-gel method is mixing the precursor in the solvent, keeping the appropriate molar ratio of reagents. The next reaction is condensation (gelation), but its separation from the hydrolysis is only symbolic as both reactions occur almost simultaneously. Condensation means joining the products of hydrolysis. The last stage is gel maturation which covers continuous changes of its structure and properties. During maturation, polycondensation is continued and the simultaneous formation of gel increases its stiffness through thickening of intermolecular contractions and reduces porosity and specific surface. Maturation causes the strength of the gel to increase. It is important for the gel to be sufficiently strong to prevent cracking at the next stage of preparation [16,17]. Structural transformations during maturation are of key importance for the drying of the gel, which is a critical stage for the final effects of synthesis. During the drying process, liquids, i.e. alcohol and water, are removed from the network of pores. It is accompanied by capillary pressure, which is responsible for generating high stresses in the gel structure. If the pores are small (<20 nm), forming capillary stresses may cause abrupt cracking of gel. The value of capillary pressure is proportionate to the interfacial surface of gel, therefore the higher the reduction of that surface during maturation, the lower the pressure and the stresses during drying. Following maturation, the gel network is stiffer and harder which contributes to better resistance against stresses and cracks during drying. Coating stabilization may be carried out by two methods, chemically and thermally, either method aims at the same target which is the removal of hydroxy groups from the surface of the gel pores. Both forms of stabilization are associated with large structural changes in the surface. Thermal stabilization of gel would require dehydration of the two forms of water. The first of these is physically adsorbed water within the gel pores. The second form consists of hydroxyl groups associated with the gel surface, which is chemically adsorbed water. During thermal stabilization as the temperature increases, the following phenomena successively occur:

>170°C—removal of the physically adsorbed water,

<400°C—reversible dehydration, irreversible decay of organic residues,

>400°C—irreversible dehydration,

700–1300°C—closing the pores, creating non-porous material.

The time of thermal stabilization should be selected in such a way that the stresses in the structure of the gel are as small as possible. Correct performance of this process results in stable gel products.

In order to deposit Al_2O_3 coating by sol-gel method, the immersion method by "dip-coater" was applied. The scheme of the station is presented in **Figure 2**. After mixing the precursor in the solvent, gelation (condensation) of the substrates occurred and the gel matured with subsequent thermal stabilization. Synthesis of Al_2O_3 coating was carried out in the following conditions:

http://dx.doi.org/10.5772/63998

- the rate of immersion and resurfacing—34mm/min,
- the temperature of stabilizing the coating—800°C.

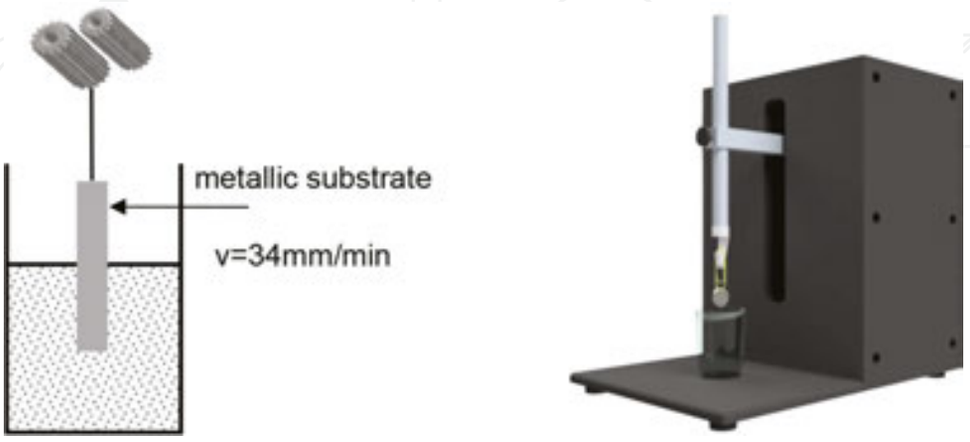

Figure 2. The scheme dip-coating process.

Multiple variations and modifications of PVD (Physical Vapour Deposition) methods are currently known that allow distinct improvement and increased operating properties of materials. These methods use a variety of physical phenomena such as vacuum cathode sputtering or evaporation of metals or metal alloys with Pa pressure reduced down from 10 to 10^{-5}. **Figure 3** shows a diagram of the elementary processes taking place during the deposition of coatings by PVD. The process of fabricating PVD coating consists of several steps, which may occur with various intensities or may be absent; sometimes they may also be amplified physically or chemically [18]:

- producing vapors of metals and alloys,
- electrical ionization of the supplied gases and metal vapors,
- crystallization of metal or metal compound from the plasma,
- condensation of plasma elements.

For the application of coatings, AlCrN target aluminum-chromium (Chromium Aluminum (AlCr) Alloy Sputtering Targets) was applied with a diameter of 100 mm, and the distance of samples from the target was 150 mm. The solid state coating material underwent vaporizing as a result of heat or ion bombardment. At the same time, nitrogen was introduced, acting as reactive gas. This resulted in the formation of a compound with the metal vapor and depositing a substrate in the form of a thin film with high adhesion. In the process, the substrates rotated at a constant speed around a few axes to obtain a uniform coating thickness. Schematic diagram of depositing the coatings by means of PVD is shown in **Figure 4**.

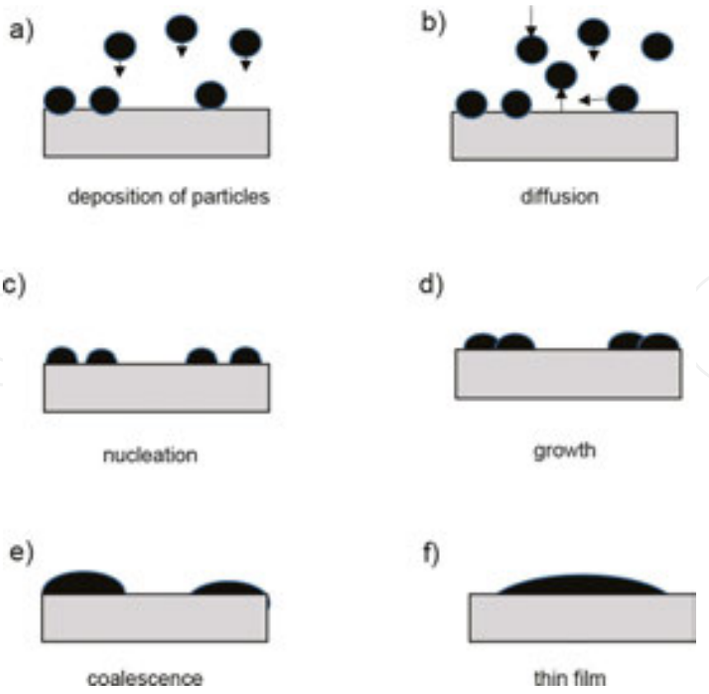

Figure 3. Elementary processes taking place during the deposition of coatings by PV.

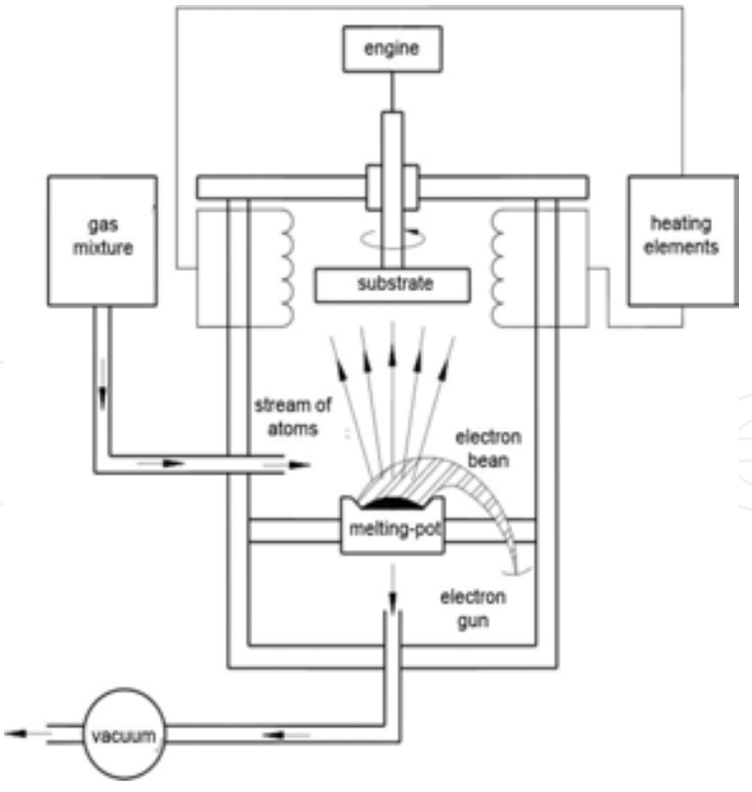

Figure 4. Schematic diagram of depositing the coatings by means of PVD.

http://dx.doi.org/10.5772/63998

The research on high-temperature oxidation was carried out at the station shown in **Figure 5**, using two types of atmospheres:

- hot air at a temperature of 700–800°C,
- atmosphere of 9% O_2+0.2% HCl+0.08% SO_2+N_2 at a temperature of 700–750°C.

The samples were heated up in the desired atmosphere with the furnace, then annealed at a given temperature, and subsequently cooled down to the room temperature. The gravimetric method was selected as a method of measuring the reaction speed; control of weight change was performed on an RADWAG precision scale with an accuracy 10^{-4} g. Trials were repeated three times and the presented test results are averaged.

Microstructural analyses were carried out by scanning electron microscopy, using a ZEISS SUPRA 35 and Hitachi S–4200 microscope equipped with EDS (energy dispersive spectroscopy) chemical composition analysis system and JSM35 JEOL microscope equipped with WDS (wavelength dispersive spectroscopy) system for analysis of the chemical composition. For research purposes, secondary electron (SE) and back-scattered electron (BSE) emissions were used. The etching of samples for structural tests was carried out using a reagent of the following chemical composition: 30ml $C_3H_6O_3$ + 15ml HNO_3 + 5ml HF. The methodology was applied for microstructural tests of both the initial-state samples and post-oxidation samples.

Figure 5. Research station.

X-ray studies of the analyzed materials were performed in X'Pert PRO PANalytical machine using filtered radiation of a lamp with a cobalt anode. X-ray phase analysis of tested materials was carried out in a Bragg-Brentano using Xcelerator strip detector and the solid angle geometry of the incidence of the primary beam (**Figure 6**) using a parallel beam collimator before the proportional detector.

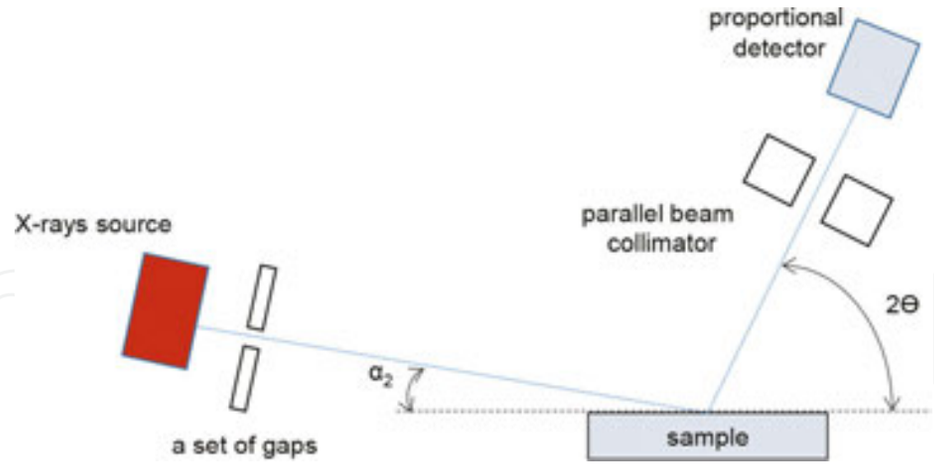

Figure 6. Goniometer arrangement for diffraction image recording in grazing incidence geometry [19].

3. Results and discussion

The microstructure of orthorhombic titanium aluminides may vary widely depending on processing methods and subsequent heat treatments [20]. The classification of orthorhombic alloys allows distinguishing typical microstructures: (a) equiaxed, (b) bimodal, (c) lamellar, and (d) lamellar with coarse secondary O laths and thick grain-boundary α_2 phase. The structure of the test alloys is presented in **Figure 7** and the type can be established as lamellar. It is a typical microstructure generated as a result of beta heat treatment of the material. The XRD (X-ray diffraction patterns) plots are shown in **Figure 8**.

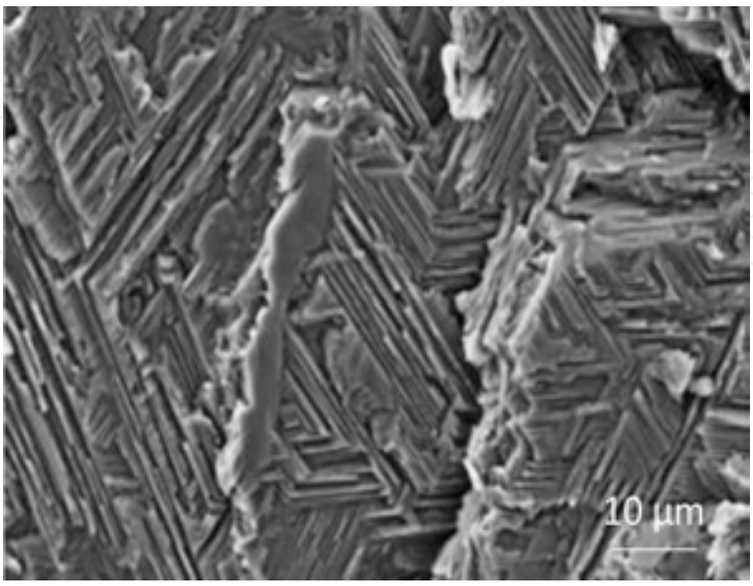

Figure 7. Microstructure of Ti-25Al-12.5Nb-6.01Mo-0.48V alloy.

http://dx.doi.org/10.5772/63998

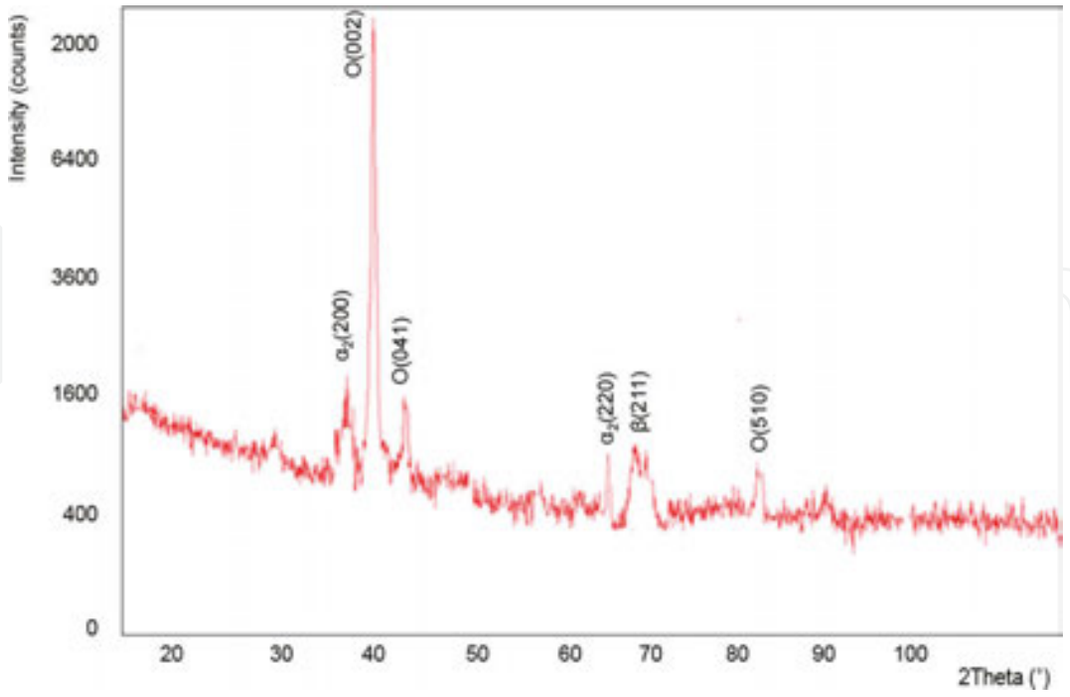

Figure 8. X-ray diffraction patterns acquired in Bragg-Brentano geometry of Ti-25Al-12.5Nb-6.01Mo-0.48V alloy.

The applied method of X-ray qualitative phase analysis performed for the deposited coatings, carried out in Bragg-Brentano geometry, confirms the presence of the respective phases in the material of the coating and substrate (**Figures 9** and **10**).

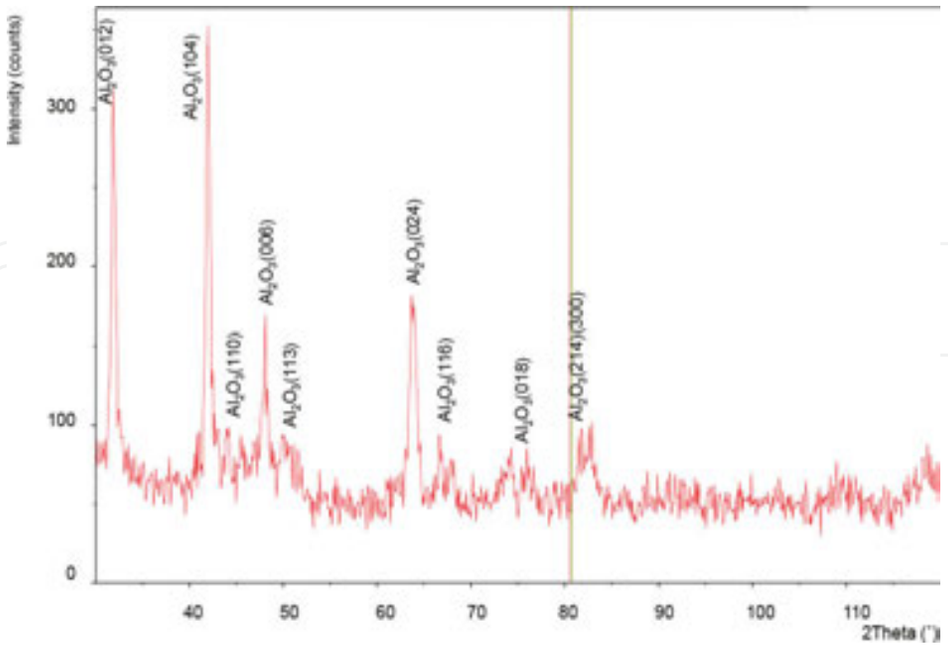

Figure 9. X-rays diffraction patterns acquired in Bragg-Brentano geometry of Al_2O_3 coatings obtained in sol-gel method.

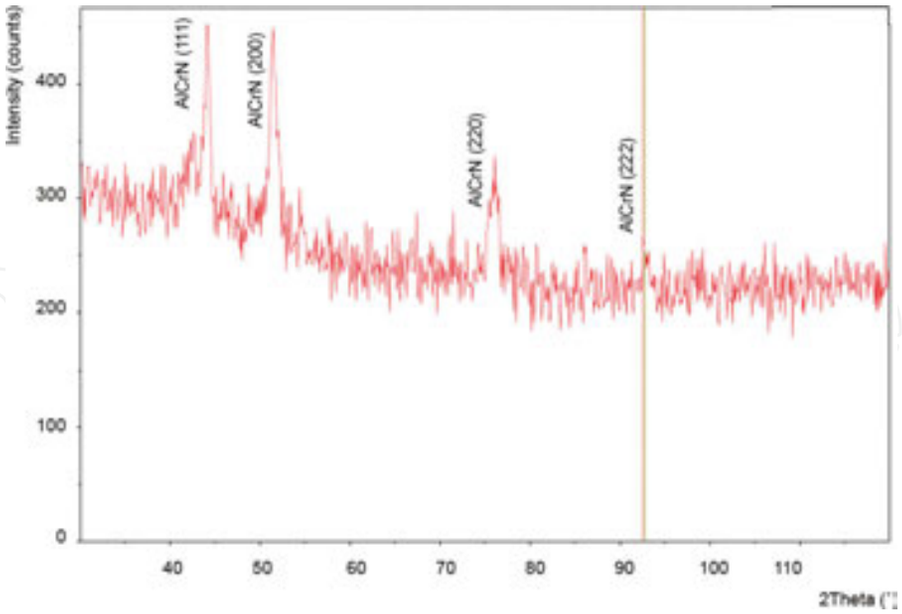

Figure 10. X-ray diffraction patterns acquired in Bragg-Brentano geometry of AlCrN coatings obtained in sol-gel method.

The course of isothermal oxidation kinetics of the alloy Ti-25Al-12.5Nb-6.01Mo-048V in the initial state and with coatings $Al_2O_3$and AlCrN deposited in air is presented in **Figure 11**. Oxidation at 700 and 800°C for 500 hours only causes mass gain, which, however, increases significantly at 800°C. The oxidation products formed exhibited adhesion to the metallic substrate for the entire duration of the test and after it. The course of the oxidation in air at 700°C exhibits rather linear course of the kinetics of oxidation, which means a continuous oxidation during exposure to high temperature, whereas during the oxidation at a temperature of 800°C, there was a change in the course of oxidation toward a course close to the parabolic. The difference in mass gain of the alloy samples oxidized at 700°C is practically insignificant, and already at 800°C significant differences were observed with definite advantage to the applied coatings. At a temperature of 700°C, the increase in mass gain occurs only at the initial period (lasting about 100 hours), and then the process slows down with mass gains on a comparable level. Samples with the coating of AlCrN show superior mass gain after oxidation in air at 700°C as compared to the alloy without coating, only up to 50th hour of oxidation and then smaller mass gains are visible. As a result, after 500 hours of isothermal oxidation, mass gains for each of the applied cases do not exceed 0.2 mg/cm^2. Oxidation in air at 800°C is characterized by decidedly larger variations; the oxide layer increases progressively, the mass gain is gradual, and therefore, it equals to approximately 1.1 mg/cm^2 for an uncoated alloy after 500 hours of oxidation. For the applied coating up to about 50th hour of oxidation, mass gains are comparable, but the differences become apparent only with elongation of exposure time. Thus, the reduction of the process rate can be determined in favor of the alloy coated with Al_2O_3, and AlCrN: a significant reduction in alloy oxidation process was observed for the coating with AlCrN, and the coating here acts as an effective protection against oxidation.

http://dx.doi.org/10.5772/63998

Apart from reducing the rate of oxidation, the scales' adhesion to the metallic substrate is also of great importance. Despite the fact that during the tests and immediately after their completion the scale formed on the coated and uncoated alloy showed good adhesion to metallic substrates, under the influence of dynamic strain loads, products near the fracture line of the uncoated alloy partially chipped already after the oxidation at a temperature of 700°C (**Figure 12**). Such chipping was not observed for coated specimens.

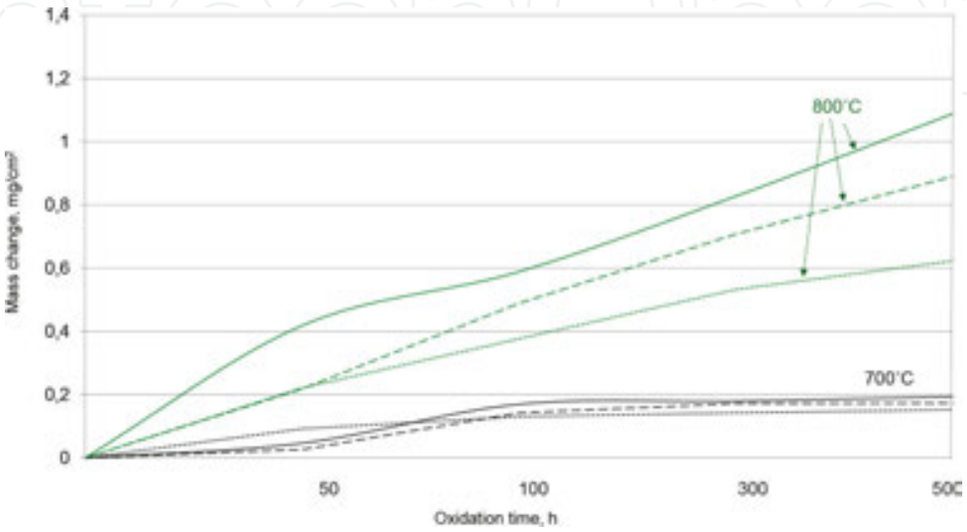

Figure 11. The mass change of Ti-25Al-12.5Nb-6.01Mo-0.48V alloy oxidized isothermally in air at 700 and 800°C (continuous curves—uncoated alloy; dashed curves—Al_2O_3-coated alloy; doted curves—AlCrN-coated alloy).

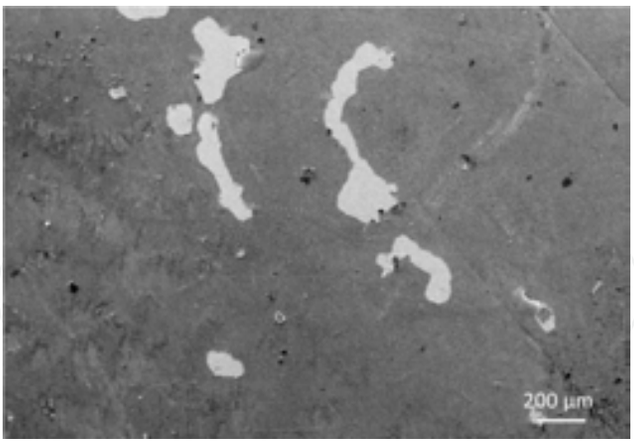

Figure 12. Fragmentary products chipped observed after oxidation in air at 700°C.

From survey of the kinetic curves during oxidation of the alloy in an atmosphere containing 9% O_2 + 0.2% HCl + 0.08% SO_2 + N_2 (**Figure 13**), it follows that already at a temperature of 700°C, and the mass gain is almost two-fold compared to the oxidation in air at the same temperature. The oxidation at 750°C displays a faster course of oxidation and increasing mass gain; however, for the uncoated alloy after 300 hours of oxidation at this temperature, a rapid

increase in the rate of oxidation is observed. The influence of coatings on the course of oxidation cannot be omitted here: both coatings promote gradual decrease of mass gain. The coated samples of the alloy have similar course up to 300th hour of oxidation, then a visible halt in the oxidation rate can be noticed as well as the decrease in mass gain. Both coatings contribute to limiting the process. In oxidation trials, the material destruction process includes the formation of oxides in heating cycles, chipping during cooling and holding in room temperature, and the total thickness of the resulting oxide layer is dependent on time and temperature of the oxidizing atmosphere. Diffusion processes activate along with the temperature rise and oxidation time.

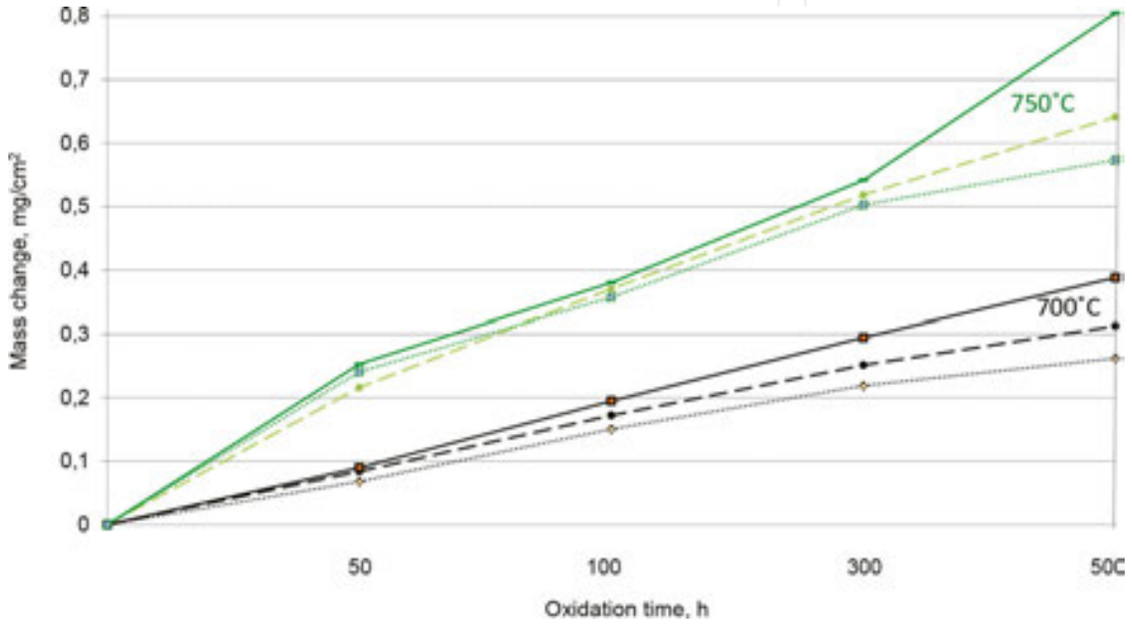

Figure 13. The mass change of Ti-25Al-12.5Nb-6.01Mo-0.48V alloy oxidized isothermally in 9% O_2+ 0.2% HCl + 0.08% SO_2+ N_2 at 700 and 800°C (continuous curves—uncoated alloy; dashed curves—Al_2O_3-coated alloy; doted curves—AlCrN-coated alloy).

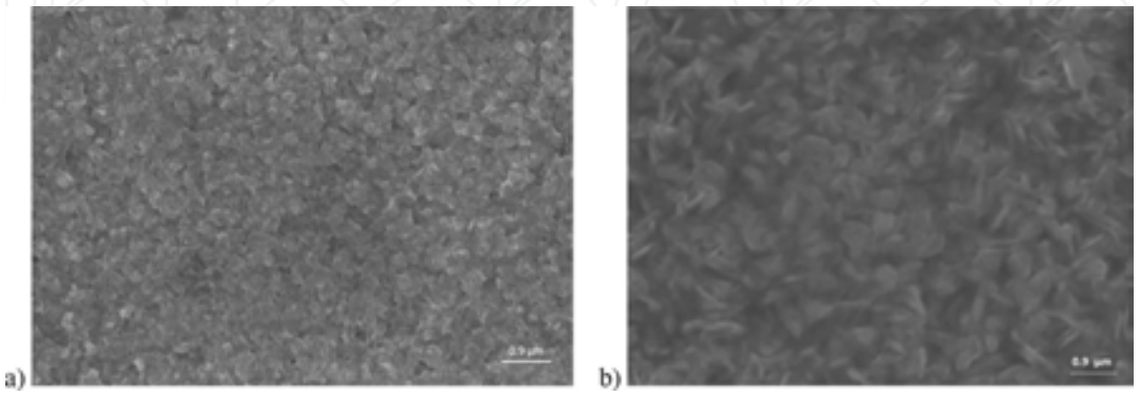

Figure 14. The surface Ti-25Al-12.5Nb-6.01Mo-0.48V after 100 (a) and 500 (b) hours of isothermal oxidation in air at 700°C.

http://dx.doi.org/10.5772/63998

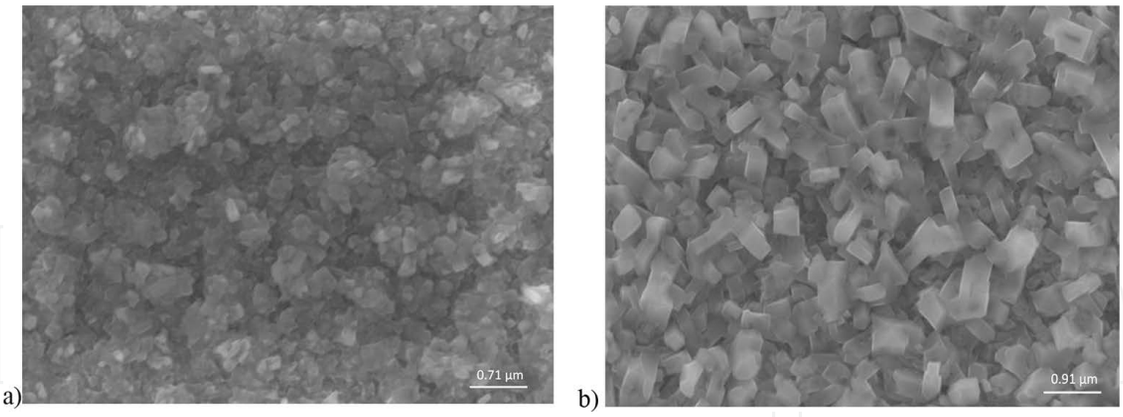

Figure 15. The surface Ti-25Al-12.5Nb-6.01Mo-0.48V after 100 (a) and 500 (b) hours of isothermal oxidation in air at 800°C.

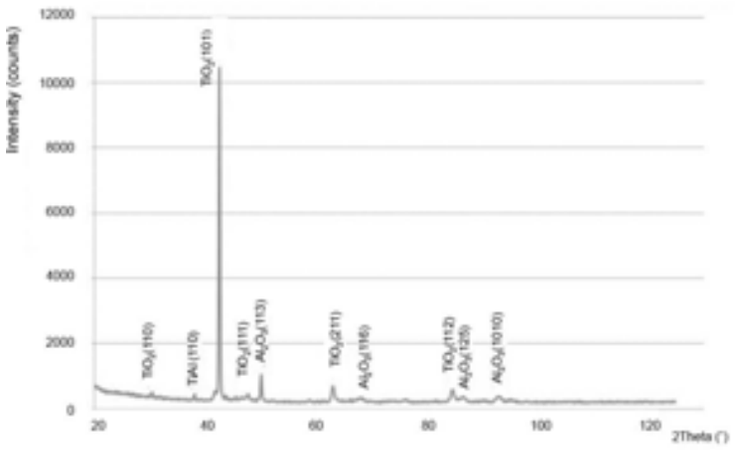

Figure 16. X-ray diffraction patterns acquired in Bragg-Brentano geometry of surface according to **Figure 14**.

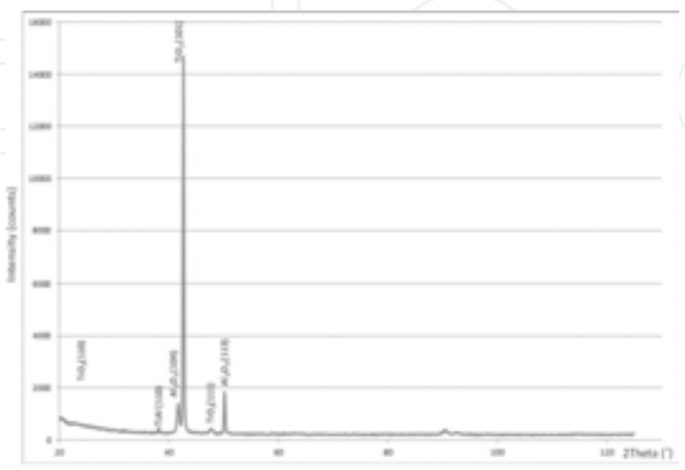

Figure 17. X-ray diffraction patterns acquired in Bragg-Brentano geometry of surface according to **Figure 15**.

Observations using SEM highlighted that the surface of the scale has a specific structure. After oxidation in air at 700°C, it is quite an irregular structure in the form of specific eruptions (**Figure 14**) loosely growing over the next sublayer, with a lamellar morphology typical of aluminum oxide. Increasing the temperature to 800°C results in the formation of the outer layer with a different morphology. The surface is formed from eruptions with the structure of irregular columnar crystallites grown in different directions (**Figure 15**). In the time interval between 50 and 100 hours, they have very small size and irregular construction. Observation of the outer surface of the products carried out after a longer time of oxidation (300–500 h) reveals that columnar rutile crystallites formed as a result of simultaneous processes of surface diffusion and out-core diffusion of titanium ions have a much larger size. These crystallites at the surface are located at different angles to each other and in relation to the surface from which they grow. The results of XRD of the surface layer (**Figures 16** and **17**) show the peaks of TiO_2; however, several Al_2O_3 phases also occur in the region of the outer oxidized layer, resulting in the formation of morphologically soft and porous oxides on the surface.

The areas of the scale's cross-section formed on the analyzed alloy are shown in **Figures 18** and **19**. The results of chemical analysis performed by the WDS in the respective characteristic regions are provided in **Tables 2** and **3**.

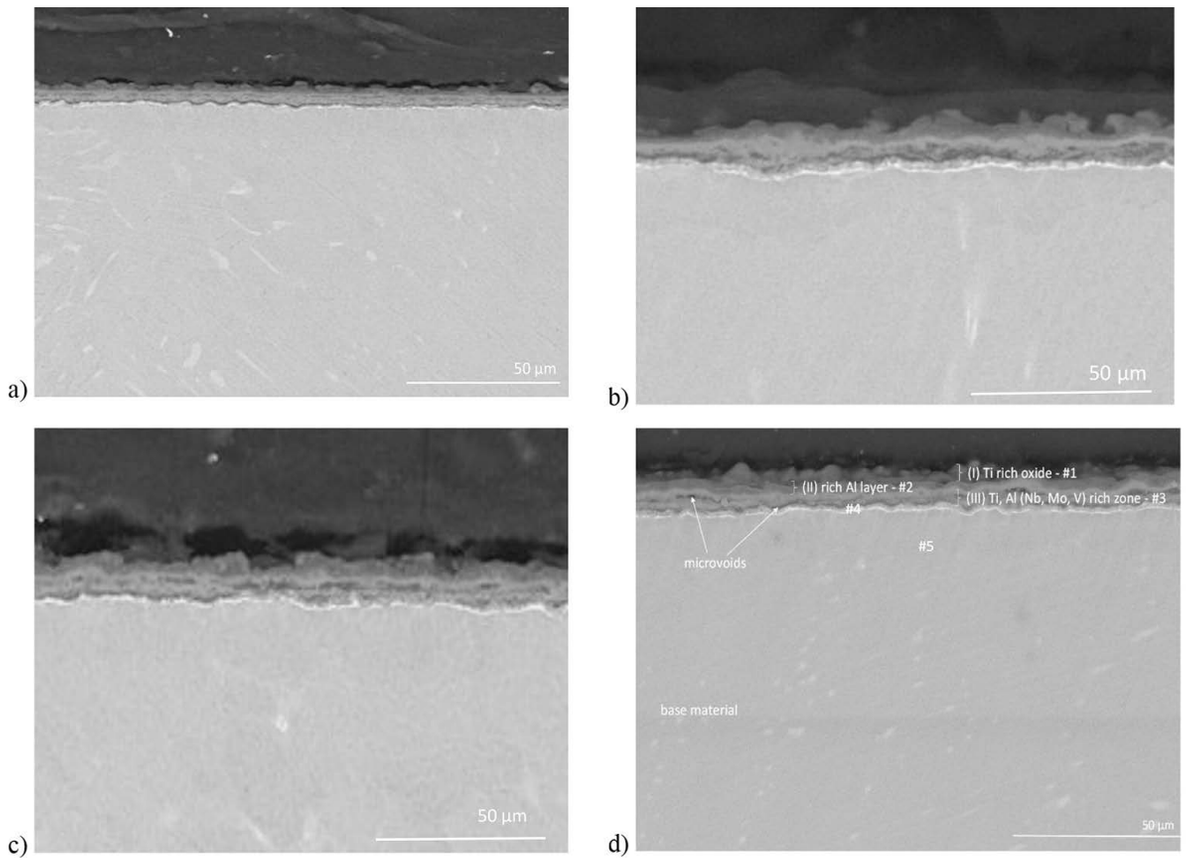

Figure 18. Cross-section of the scale formed on Ti-25Al-12.5Nb-6.01Mo-0.48V after 50 (a); 100 (b); 300 (c); 500 (d) hours of isothermal oxidation in air at 700°C.

http://dx.doi.org/10.5772/63998

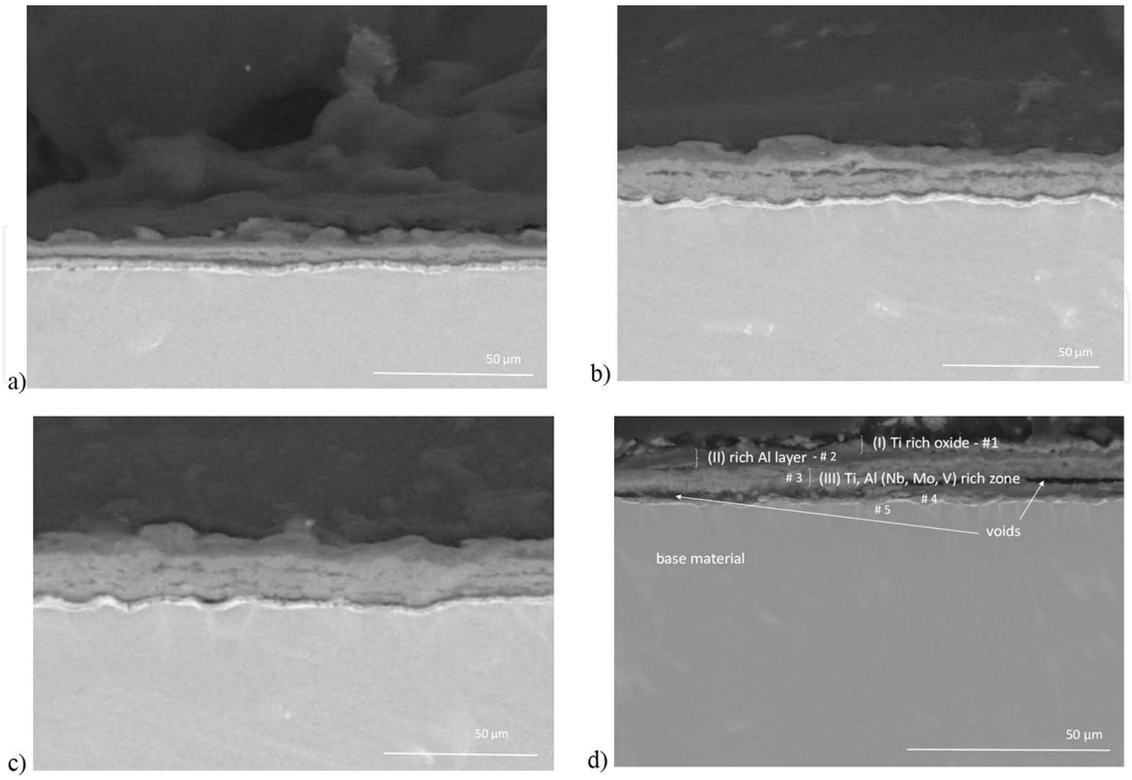

Figure 19. Cross-section of the scale formed on Ti-25Al-12.5Nb-6.01Mo-0.48V after 50 (a); 100 (b); 300 (c); 500 (d) hours of isothermal oxidation in air at 800°C.

	NO	Al	Nb	Ti	Mo	V	
#1	0.00	54.40	12.46	5.35	27.79	–	–
#2	0.00	53.95	31.24	0.36	13.27	0.61	0.47
#3	0.00	51.58	19.72	2.37	25.48	0.85	–
#4	14.24	18.46	18.73	10.93	35.47	1.81	0.36
#5	3.70	7.63	25.27	11.07	48.94	2.97	0.42

Table 2. WDS-analysis (at.%) of locations labeled in **Figure 18d**.

	N	O	Al	Nb	Ti	Mo	V
#1	0.00	59.49	11.84	4.85	23.82	–	–
#2	0.00	55.62	37.27	0.72	5.83	0.56	–
#3	0.00	54.98	21.00	1.98	20.87	0.80	0.37
#4	16.60	19.00	20.82	8.91	33.35	1.20	0.12
#5	2.44	11.79	26.96	10.98	44.44	3.01	0.38

Table 3. WDS-analysis (at.%) of locations labeled in **Figure 19d**.

Basically, the scale formed showed the concentration of fine pores and a layered structure made of alternate layers. This is due to the fact that Ti has been selectively oxidized to TiO_2, under which the elements Nb and Al were relatively enriched. Then the oxygen diffusing through a layer rich in TiO_2 reacted with Nb and Al, which allowed for the formation of a layer most likely enriched in $AlNbO_4$. Under the layer rich in $AlNbO_4$, Ti is enriched again. Therefore, a multilayer scale is formed consisting of alternating layers rich in TiO_2 and $AlNbO_4$. It was observed that oxygen and nitrogen were present in the interface between the oxide scale and the metallic substrate, and subsurface embrittlement caused by formation of the nitride layer and the penetration of air/nitrogen was evident (microvoids).

The analyzed alloy is characterized by the formation of a scale as the reaction product and the formation of the diffusion area of interstitial elements in the metallic substrate. Oxide layers formed during annealing consist of a few characteristic sublayers, however, with a similar structure and chemical composition. External sublayer (I) existing at the phase boundary with an oxidant (air) consists predominantly of rutile accumulations also containing Al oxides. Middle sublayer (II) forms a band extending parallel to the oxidized surface and characterized by the fact that BSE observation gives gray-graphite contrast, which is not heterogeneous. This band has a lot of Al_2O_3 but little TiO_2. The fact that these oxides come separately causes the non-uniformity of contrast. Aluminum cations which diffuse out-core (slower than Ti) form Al_2O_3 with the oxygen. A protective layer will be formed in the reaction products only when it exclusively contains Al_2O_3. The Al_2O_3 layer formed is heterogeneous and not compact. Its content also includes TiO_2 rutile, however, in lesser amount. The presence of even a small amount of TiO_2 in the sublayer rich in Al_2O_3 enables a two-way diffusion, thus resulting in the growth of the product on the outer surface and at the interface product-metallic substrate. The inner sublayer (III) contains comparable amounts of Al_2O_3 and TiO_2. Moreover, it contains oxides of alloying elements included in the composition of the analyzed alloy. Microvoids occur between this sublayer and the metallic substrate. As the temperature rises, the number of microvoids rises, as well as their size and their tendency to join is observed. The structure of this phase boundary determines the possibility of scale buckling during cooling. Thus, Nb, Mo, and V co-create oxides in virtually any sublayer. It can be noticed that in the region of product-substrate micropores' boundary is actively developing. Thus, out-core diffusion of metal ions is accompanied by the increase in concentration of vacancies at the interface between the substrate-product, until a break in cohesion occurs in nano-regions and then micro-regions. Compressive stresses generated upon oxidation and cooling the sample down to the room temperature cause the buckling of the layer and its removal from the substrate. Diffusion processes taking place on the flat interface cause the coalescence of vacancies, the formation of microvoids, and their joining into bands. Due to the fact that the decohesion of oxide fragments from the substrate requires high shear stresses at the interface, the "weakening" of phase boundary by the microvoids promotes the process of buckling. Buckling, in turn, induces a tensile stress and micro-cracks in the layer separated from the surface, consequently causing cracking, crushing, and chipping of scale fragments. Phase separation at the interface of the scale/metal substrate occurs as a result of the tensile stresses generated in direction tangential to the interface of the scale/metal substrate and compressive stresses in the transverse direction to the border of the phases. As a result of the impact of both types of stresses, a local separation

http://dx.doi.org/10.5772/63998

of the scales from the surface of the substrate material occurs. The result is the formation of discontinuities in scale adhesion to the metal substrate. This can cause increased susceptibility to detachment of the scale during oxidation.

In the initial period of scale growth, poor tensile stresses formed on the alloy oxidized at 700°C in a direction tangential to the interface oxide/metal substrate and compressive stresses in a direction transverse to the interfacial oxide/metal substrate. At the same time, small voids began to form in the region of the interface of scale/substrate. The increase of oxidation temperature (up to 800°C) leads to increased stresses and expansion of discontinuity at the interface of oxide/metal substrate. After 500 hours of oxidation, voids widened creating small cracks in the scale, which decreases protective properties of the scale.

The result of the oxidation of the alloy Ti-25Al-12.5Nb-6Mo-0.48V in the atmosphere of 9% O_2 + 0.2% HCl + 0.08% SO_2+N_2 is the formation of reaction products characterized by completely different morphology than that observed in previous studies. Oxidation in such conditions causes the formation of specific eruptions on the outer surface, under which another sublayer is revealed (**Figures 20** and **21**).

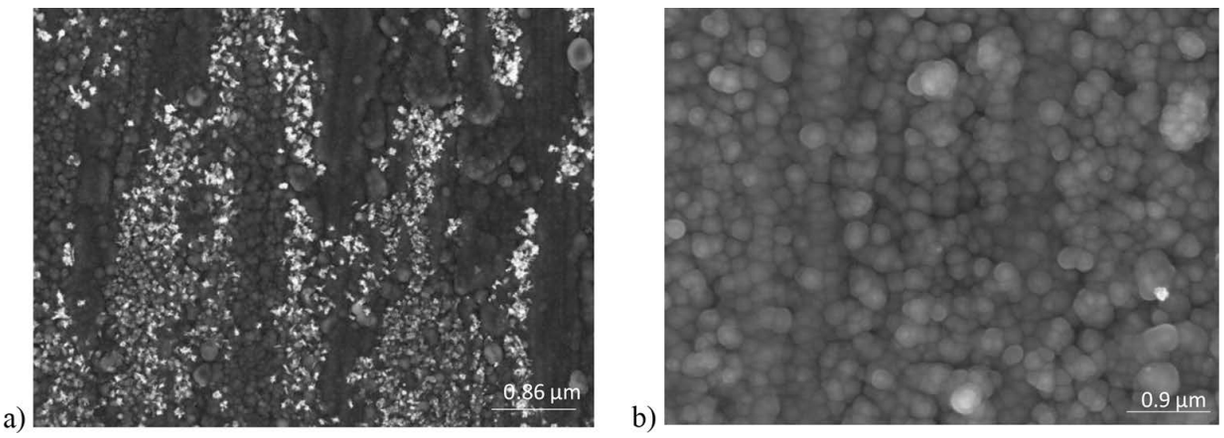

Figure 20. The surface Ti-25Al-12.5Nb-6.01Mo-0.48V after 100 (a) and 500 (b) hours of isothermal oxidation in 9% O_2+ 0.2% HCl + 0.08% SO_2+ N_2 atmosphere at 700°C.

Analysis of the chemical composition of the outer surface of the scale (**Figure 22**) proved that the forming outer layer is composed mainly of the mixture of oxides Al and Ti. Nb and traces of S were observed on the oxidized surface. Metallographic examination showed that the forming oxides grow with increasing temperature and time of the process. Temperature rise of the process causes the formation of scale with distinct whisker-like morphology of oxides (**Figure 21**) which effectively hinders protection of the alloy against the impact of corrosive environment in the next stages of the test. In consequence, after 500 hours of oxidation at a temperature of 750°C, the surface is covered with columnar eruptions irregularly arranged relative to each other (**Figure 21d**).

The examination of cross-sectional metallographic specimens after experiment in the atmosphere of 9% O_2+ 0.2% HCl + 0.08% SO_2+ N_2 allowed revealing the multi-layered nature of the scale (**Figure 23**) with distinct separation of borders between the sublayers. The sequence of

products and their morphology is essentially not different from the products obtained during the oxidation in air.

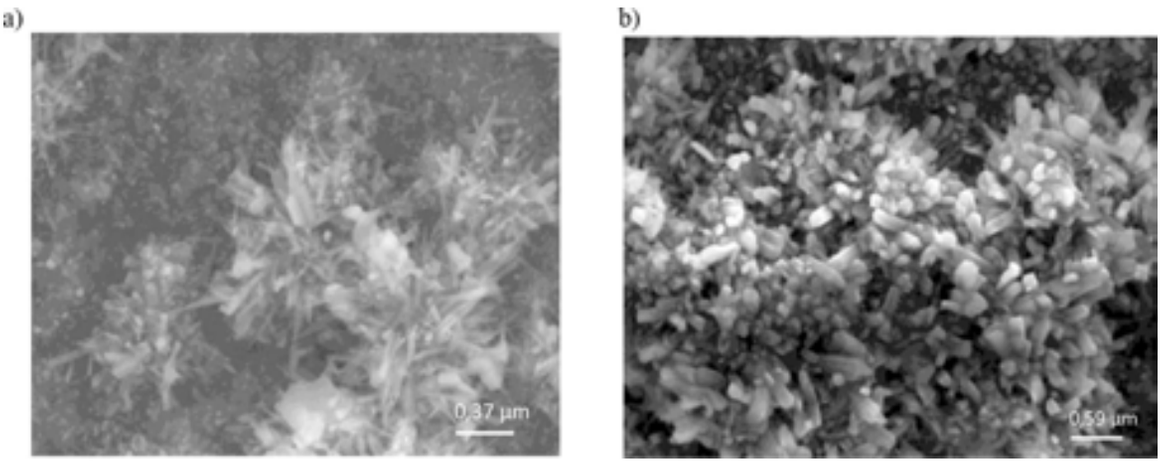

Figure 21. The surface Ti-25Al-12.5Nb-6.01Mo-0.48V after 100 (a) and 500 (b) hours of isothermal oxidation in 9% O_2+ 0.2% HCl + 0.08% SO + N_2 atmosphere at 800°C.

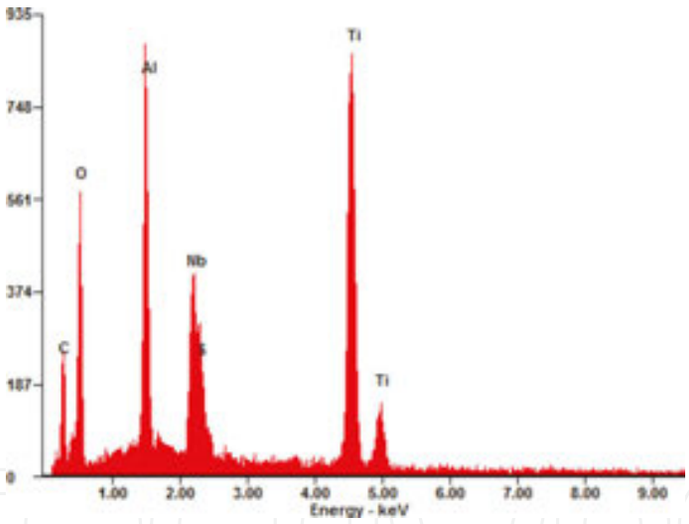

Figure 22. EDX analysis results in place according to **Figure 21**.

Based on the chemical composition analysis of the layers, it was determined that similar to oxidation in air, directly under the outer layer (I) containing mainly Ti and Al, a sublayer is formed with a dominance of Al (II), and another mixed sublayer rich in titanium oxides, aluminum, and alloying elements (III) with a dominance of Ti. The detailed chemical composition of respective layers is presented in **Tables 4** and **5**. It is noteworthy that the layer of corrosion products formed in the atmosphere of 9% O_2+ 0.2% HCl + 0.08% SO_2+ N_2 already at 700°C is characterized by porous structure (**Figure 23**). Therefore, it does not provide sufficient protection against the destructive impact of corrosive environment. Lower cohesion of the scale facilitates bidirectional transport of metal ions and oxidants (O and N), causing the

product to grow faster on both phase interfaces, i.e. product-substrate interface and product-oxidant interface.

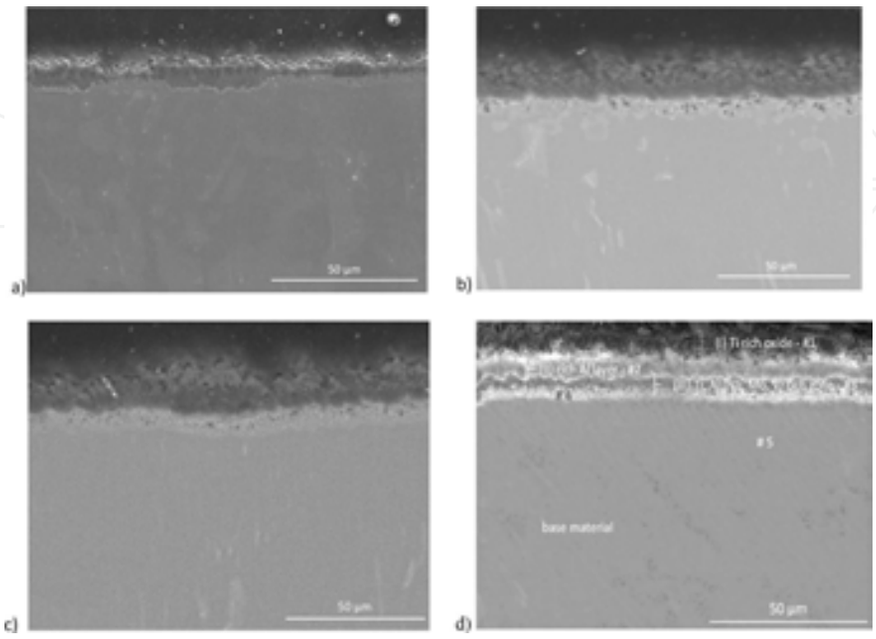

Figure 23. Cross section of the scale formed on Ti-25Al-12.5Nb-6.01Mo-0.48V after 50 (a); 100 (b); 300 (c) and 500 (d) hours of isothermal oxidation in 9% O_2+ 0.2% HCl + 0.08% SO_2+ N_2 atmosphere at 700°C.

	N	O	S	Al	Nb	Ti	Mo	V
#1	0.00	49.99	3.21	14.31	5.78	26.71	0.00	0.00
#2	0.00	55.74	0.00	36.17	0.97	6.29	0.71	0.12
#3	0.00	44.61	7.91	18.92	1.93	24.76	1.02	0.85
#4	18.21	19.54	0.00	17.65	9.65	32.15	2.15	0.65
#5	3.81	10.24	0.00	25.93	13.12	43.30	3.31	0.29

Table 4. WDS-analysis (at.%) of locations labeled in **Figure 23d**.

	N	O	S	Al	Nb	Ti	Mo	V
#1	0.00	56.01	4.57	10.07	4.21	25.14	0.00	0.00
#2	0.00	54.35	0.00	37.86	1.19	5.64	0.51	0.45
#3	0.00	43.47	6.27	21.53	2.04	25.37	0.72	0.60
#4	13.74	20.78	0.00	21.22	8.73	33.17	1.85	0.51
#5	2.37	8.56	0.00	27.47	10.95	47.22	2.84	0.59

Table 5. WDS-analysis (at.%) of locations labeled in **Figure 24d**.

SEM observations showed that the scale has a compact, homogeneous structure, with numerous small discontinuities (**Figures 23** and **24**). During oxidation in air, the scale composed of characteristic eruptions forms on the surface, and the scale which is formed during the oxidation in the model atmosphere is characterized by the presence of needle-shaped oxides growing on its surface and expanding as the oxidation time increases. During the oxidation in air, it was observed that the layer closest to the substrate is characterized by irregular structure, with pits inside material and extensive discontinuity propagating between the layers. On the other hand, a thicker layer formed during the oxidation in an aggressive atmosphere has visible and noticeable pores. In this layer, relatively large amount of sulfur and chlorine is also noticeable from the viewpoint of corrosion (**Tables 4** and **5**).

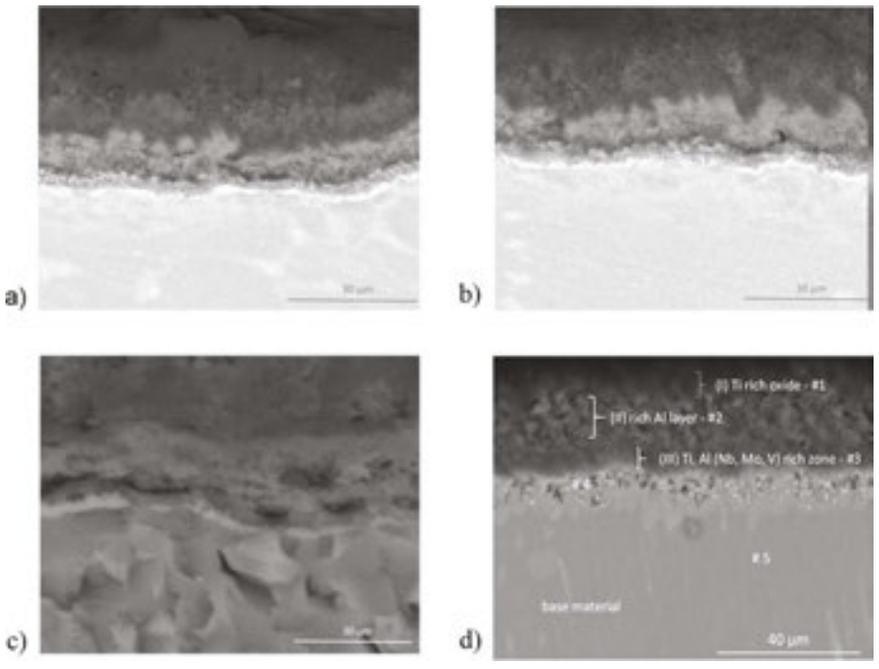

Figure 24. Cross section of the scale formed on Ti-25Al-12.5Nb-6.01Mo-0.48V after 50 (a); 100 (b); 300 (c) and 500 (d) hours of isothermal oxidation in 9% O_2+ 0.2% HCl + 0.08% SO_2+ N_2 atmosphere at 800°C.

Most likely, such course of reaction is caused by reactivity of sulfur vapors which belong to the most aggressive ones as regards corrosion due to the fact that sulfur reacts with almost all metallic elements. The similarity of morphological structure between sulfide scale and oxide scale results from the corresponding mechanism of its growth (outward diffusion of alloying elements). The difference lies in better developed porous outer layer and larger sizes of grains forming the outer compact layer. Despite the similarities, the mechanism of sulfide scale growth is more complicated than oxide scale growth. It follows from a larger number of thermodynamically stable metal sulfides as compared to oxides, and also the fact that the structure of defects in sulfides is more complicated and yet to be sufficiently explained. Despite the fact that the mechanism of sulfur corrosion has been well researched, the difficulties posed in these experiments cause that analysis of heterogeneous reaction occurring at high temperatures in atmospheres with sulfur compounds leave many unexplained correlations. Other

factors complicating the sulfidation of metals and alloys are the changes occurring in metal sulfides. Sulfides of common metals are less stable thermodynamically, have lower melting points, and display significant deviation from stoichiometry as compared to corresponding oxides. The course of corrosion of T Ti-25Al-12.5Nb-6.01Mo-0.48V alloy in the atmosphere of $9\%O_2+0.2\%HCl+0.08\%\ SO_2+N_2$ may be compared to corrosion occurring in air. However, in the environment containing even such small amounts of sulfur, metallic materials resistant to high-temperature oxygen corrosion may undergo degradation, which can lead to breakaway corrosion.

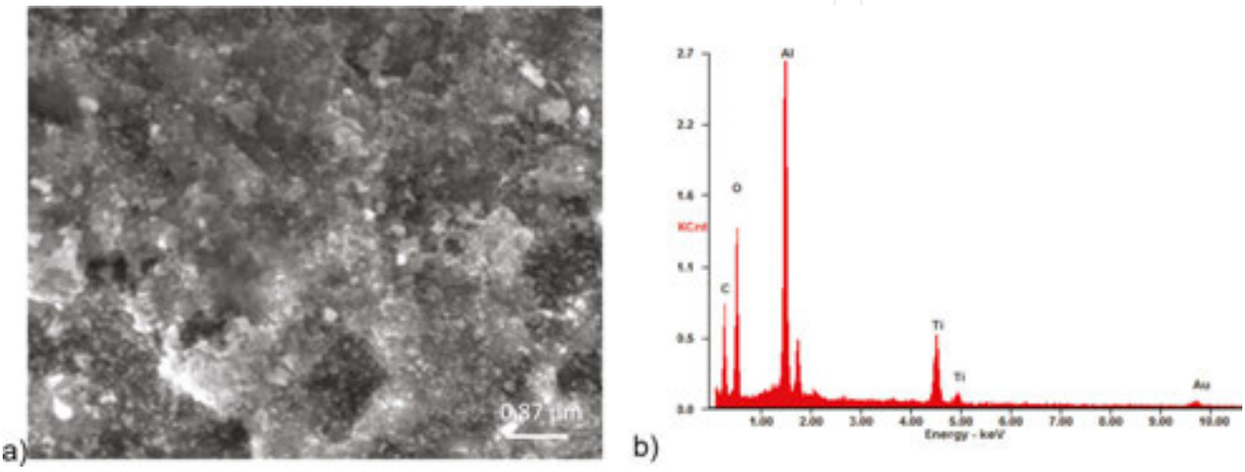

Figure 25. The surface Ti-25Al-12.5Nb-6.01Mo-0.48V coated Al_2O_3 after isothermal oxidation in air (a); EDX analysis results in place according to **Figures 25a** (b).

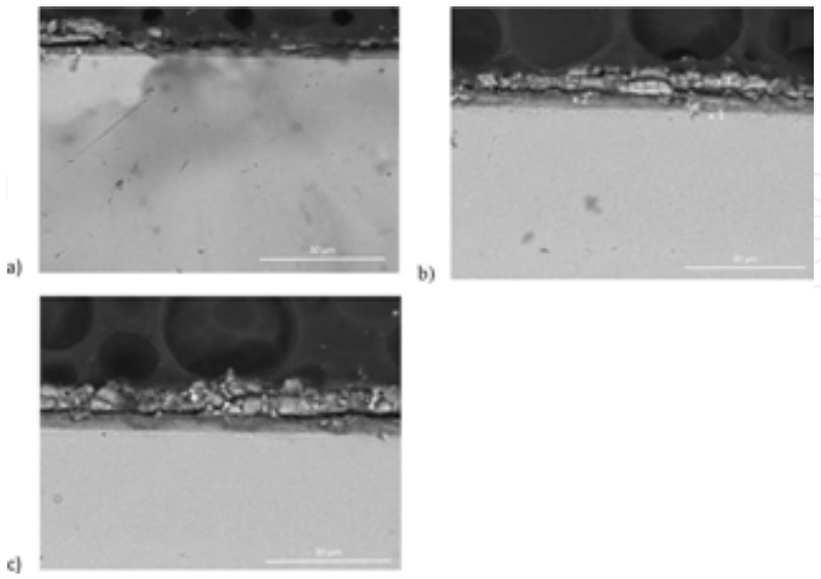

Figure 26. Cross-section of the scale formed on Ti-25Al-12.5Nb-6.01Mo-0.48V coated Al_2O_3 after 100 (a); 300 (b) and 500 (c) hours of isothermal oxidation in air at 700°C.

The morphological structure of the scale formed upon the oxidation of the alloy coated with Al_2O_3 (**Figures 26 – 28**) shows a difference in the outer surface construction. A characteristic feature of the surface is that it is characterized by the finest construction. The outer layer is therefore made of quite a porous scale that is visible over the entire surface of the oxidized alloy independent of the temperature and oxidation time. It can be concluded that the pellets observed on the surface consist mainly of Al_2O_3 and to a lesser extent, TiO (**Figure 26**). Due to diffusion processes occurring at high temperature, the coating of Al_2O_3 undergoes transformation; compact and dense initial Al_2O_3 coating is dissolved, and its place is taken by a porous scale. Analysis of the chemical composition shows mainly the occurrence of small amounts of Ti (**Figure 25**), which diffuses directly from the substrate due to the impact of high temperature. Elongation of the oxidation time causes that under the porous outer layer other sublayers are formed characterized by the presence of regions of high heterogeneity, discontinuity and buckling (**Figures 26** and **28**). The scale formed is multi-layered; in particular regions, detailed analysis of the composition was performed (the results are presented in **Tables 6** and **7**). Interfaces between the individual layers are clearly visible, as well as the resulting discontinuities along the scale, that grow as the oxidation time increases.

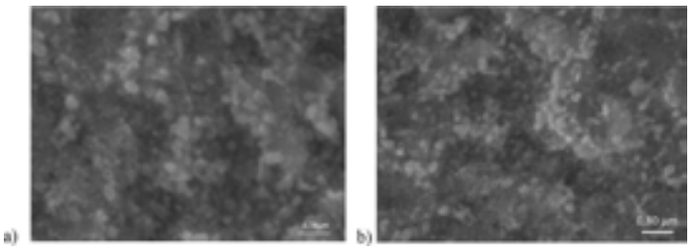

Figure 27. The surface Ti-25Al-12.5Nb-6.01Mo-0.48V coated Al_2O_3 after 100 (a) and 500 (b) hours of isothermal oxidation in air at 800°C.

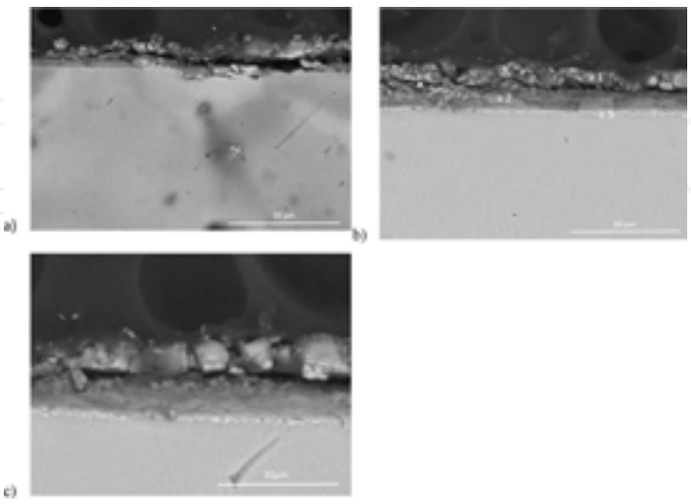

Figure 28. Cross section of the scale formed on Ti-25Al-12.5Nb-6.01Mo-0.48V coated Al_2O_3 after 100 (a); 300 (b) and 500 (c) hours of isothermal oxidation in air at 800°C.

http://dx.doi.org/10.5772/63998

During the oxidation of the alloy, the dissociation of the Al_2O_3 coating occurs, and the oxygen diffusing to the substrate from the coating reacts with Ti and forms TiO compounds during the oxidation process. Cross-sectional metallographic specimens show that the thickness of the scale is homogeneous, but it increases with the rise of the oxidation temperature. After partial wear and dissociation of the original Al_2O_3 coating, the in-core diffusion of oxygen and ex-core diffusion of Ti accelerates scale growth.

	N	O	Al	Nb	Ti	Mo	V
#1	–	48.12	44.61	–	7.27	–	–
#2	–	25.92	38.21	2.13	33.74	–	–
#3	–	23.11	26.94	17.32	29.98	2.31	0.34

Table 6. WDS-analysis (at.%) of locations labeled in **Figure 27b**.

	N	O	Al	Nb	Ti	Mo	V
#1	–	46.91	45.14	–	7.95	–	–
#2	–	28.11	41.06	1.97	28,86	–	–
#3	–	22.97	27.03	16.53	29.86	2.97	0.64

Table 7. WDS-analysis (at.%) of locations labeled in **Figure 28b**.

During the oxidation of the alloy with the coating, probably the dissociation of Al_2O_3 coating occurs, and the oxygen diffusing to the substrate from the coating reacts with Ti and forms TiO compounds during the oxidation process. Probably, niobium originating from the substrate of the alloy does not react with Al_2O_3 layer, which is confirmed by tests carried out by Mader and Rühler [21] who established that no reaction layer is formed between the Nb and Al_2O_3 in the high-temperature oxidation. Al_2O_3 compound reacts with Ti because of the high solubility of oxygen in titanium and occurring diffusion of oxygen to the metallic substrate. During the oxidation of this alloy, it is noted that in this case also a light layer is formed (interface between the oxide scale and the metallic substrate), which was identified as the region rich in Nb. Due to the inter-diffusion that occurs between the coating layer and the substrate of Ti-25Al-12.5Nb-6.01Mo-0.48V alloy, it is the original Al_2O_3 layer that was transformed. A small amount of Ti was found that diffused from the alloy O-Ti_2AlNb due to the impact of high temperature. In this case, the ongoing isothermal oxidation resulted in the formation of oxide lumps on the surface of the sample. It can be concluded that the lumps consist essentially of Al_2O_3 and TiO_2 to a lesser extent. The source of these recognizable peaks is the oxidized O-Ti_2AlNb alloy. So the oxidation of the metallic substrate of alloy-Ti_2AlNb

occurred under a layer of Al_2O_3 coating. The compact and dense initial Al_2O_3coating dissolved and its place was taken by a porous scale. From the cross-cut metallographic specimens, it can be seen that the thickness of the oxide scale is uniform. Lumps in the outer layer consist primarily of Al_2O_3. After partial wear and dissociation of the original Al_2O_3 coating, the in-core diffusion of oxygen and ex-core diffusion of Ti accelerates scale growth.

During the oxidation of tested alloy coated Al_2O_3 in an atmosphere containing 9% O_2+ 0.2% HCl + 0.08% SO_2+ N_2, a pronounced impact of the oxidizing environment on the intensity of high-temperature corrosion was observed.

Both during the oxidation of the alloy coated with Al_2O_3 in the air and in the model atmosphere of 9% O_2+ 0.2% HCl + 0.08% SO_2+ N_2, the outer layer is made of quite a porous scale that is visible over the entire surface of the oxidized alloy independent of the temperature and oxidation time. However, due to the diffusion processes in the aggressive atmosphere, well developed oxide lumps are formed on the surface of the sample (**Figures 29** and **32**), whose size increases as the oxidation time increases. The surface is characterized by the presence of regions of high heterogeneity, discontinuity, and buckling. There is occurrence of chlorine and sulphur compounds on the outer surface of the scale (**Figure 30**). In general, the scale formed during oxidation in air has a similar structure, but it is much thinner. Tests carried out on transverse sections (metallographic specimens) show that the oxidation products exhibit a multilayered structure with discontinuities of high porosity. Three specific areas can be distinguished: internal, external and central (**Figures 31** and **33**), while chlorine and sulphur decreases inwardly from the outer layer, and in the layer directly adjacent to the material (Item 3, **Tables 8** and **9**) compounds of S and Cl were not found. Oxidation in the model atmosphere causes buckling and separation of scale from the substrate, which leads to the conclusion that the applied coating in this case was not a sufficient protection against the exposure to oxidizing environment.

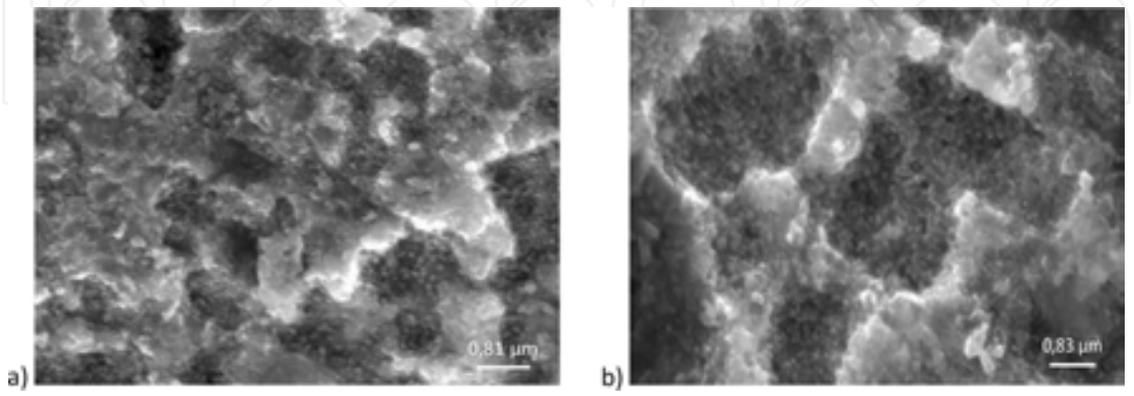

Figure 29. The surface Ti-25Al-12.5Nb-6.01Mo-0.48V coated Al_2O_3 after 100 (a) and 500 (b) hours of isothermal oxidation in 9% O_2+ 0.2% HCl + 0.08% SO_2+ N_2 atmosphere at 700°C.

http://dx.doi.org/10.5772/63998

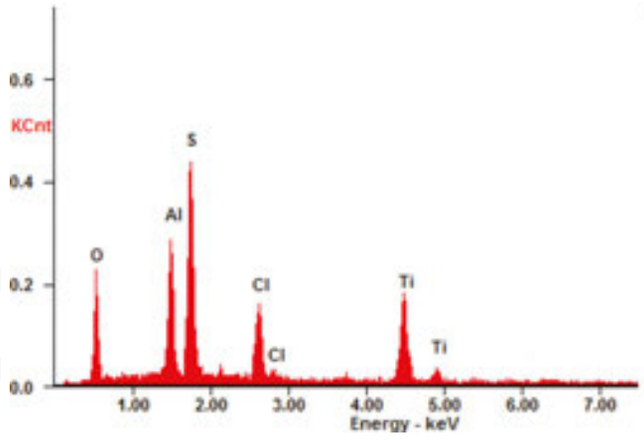

Figure 30. EDX analysis results in place according to **Figure 29**.

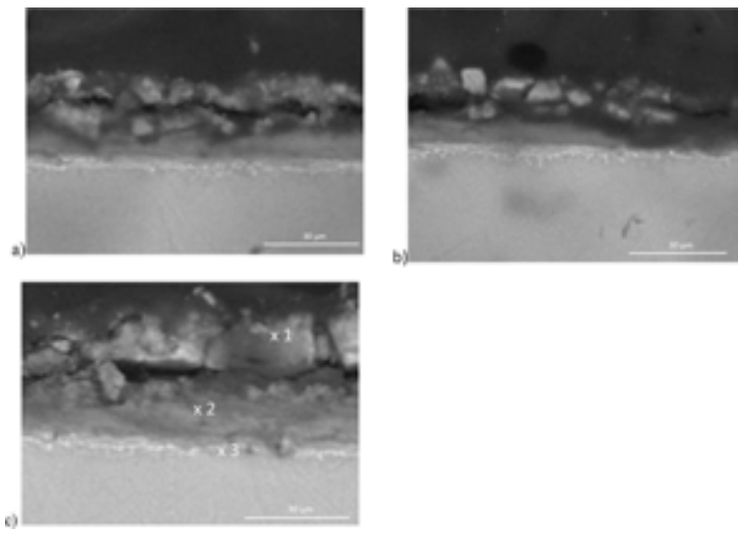

Figure 31. Cross section of the scale formed on Ti-25Al-12.5Nb-6.01Mo-0.48V coated Al_2O_3 after 100 (a); 300 (b) and 500 (c) hours of isothermal oxidation in 9% O_2+ 0.2% HCl + 0.08% SO_2+ N_2 atmosphere at 700°C.

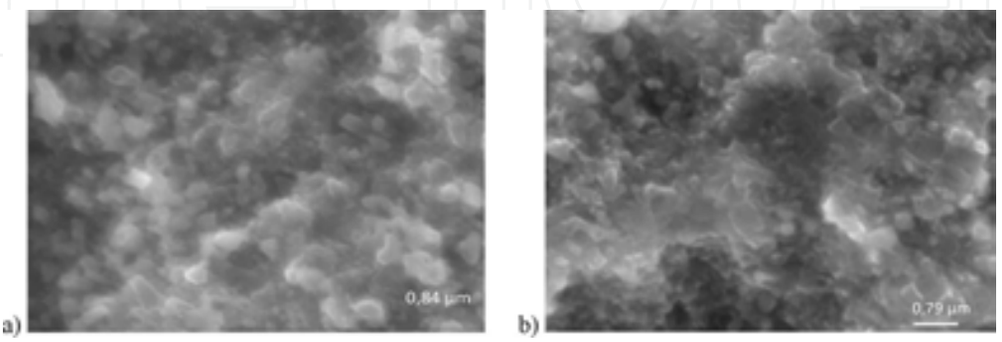

Figure 32. The surface Ti-25Al-12.5Nb-6.01Mo-0.48V coated Al_2O_3 after 100 (a) and 500 (b) hours of isothermal oxidation in 9% O_2+ 0.2% HCl + 0.08% SO_2+ N_2 atmosphere at 750°C.

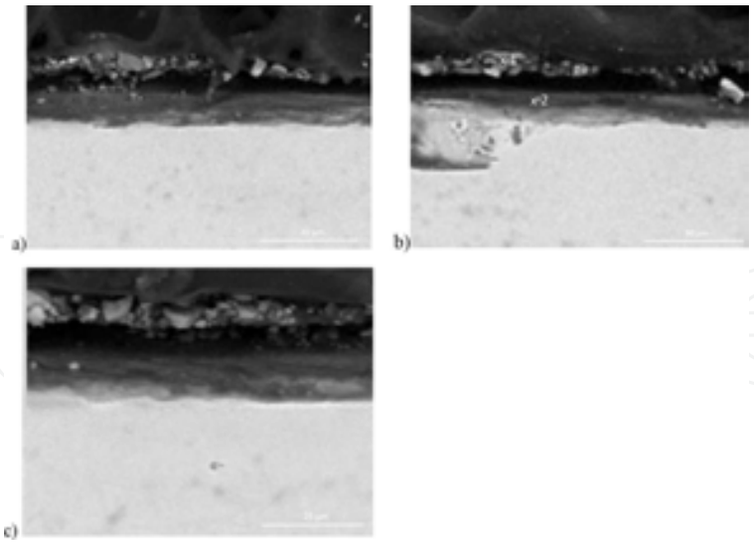

Figure 33. Cross-section of the scale formed on Ti-25Al-12.5Nb-6.01Mo-0.48V coated Al_2O_3 after 100 (a); 300 (b) and 500 (c) hours of isothermal oxidation in 9% O_2+ 0.2% HCl + 0.08% SO_2+ N_2 atmosphere at 750°C.

	O	Al	Nb	Ti	Mo	V	S	Cl
#1	37.55	43.68	–	12.78	–	–	1.67	4.32
#2	28.04	36.21	3.53	30.96	–	–	0.06	1.20
#3	21.36	27.76	17.32	30.27	3.01	0.28	–	–

Table 8. WDS-analysis (at.%) of locations labeled in **Figure 31c**.

	O	Al	Nb	Ti	Mo	V	S	Cl
#1	37.69	41.21	–	14.12	–	–	2.03	4.95
#2	34.65	38.74	5.27	19.99	–	–	0.57	0.78
#3	19.54	28.27	15.97	32.20	3.49	0.53	–	–

Table 9. WDS-analysis (at.%) of locations labeled in **Figure 33b**.

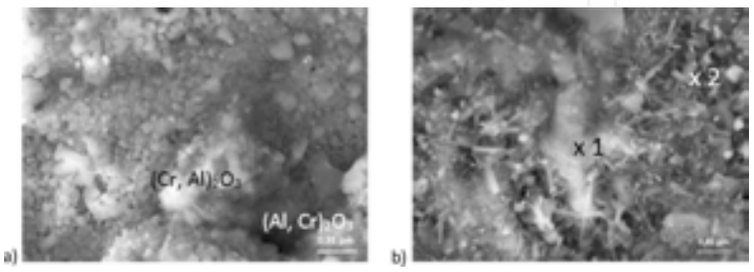

Figure 34. The surface Ti-25Al-12.5Nb-6.01Mo-0.48V coated AlCrN after 100 (a) and 500 (b) hours of isothermal oxidation in air at 700°C.

http://dx.doi.org/10.5772/63998

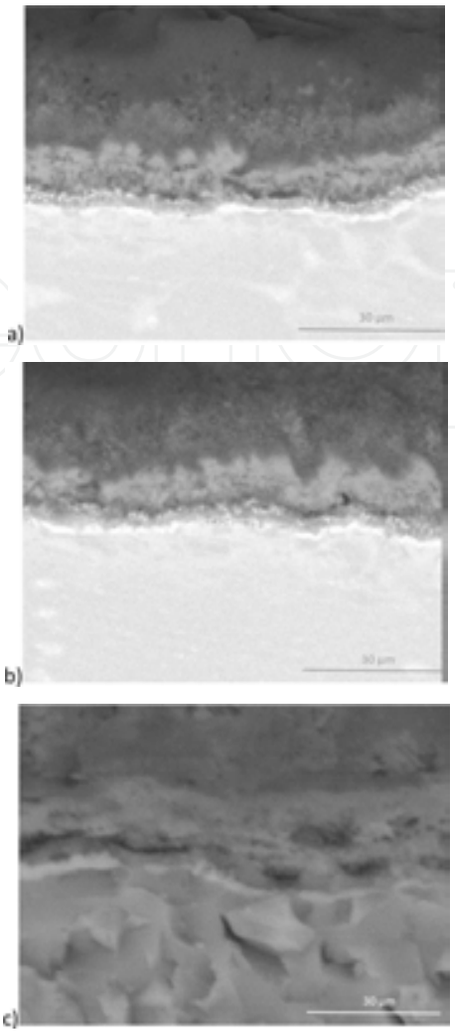

Figure 35. Cross section of the scale formed on Ti-25Al-12.5Nb-6.01Mo-0.48V coated AlCrN after 100 (a); 300 (b) and 500 (c) hours of isothermal oxidation in air at 700°C.

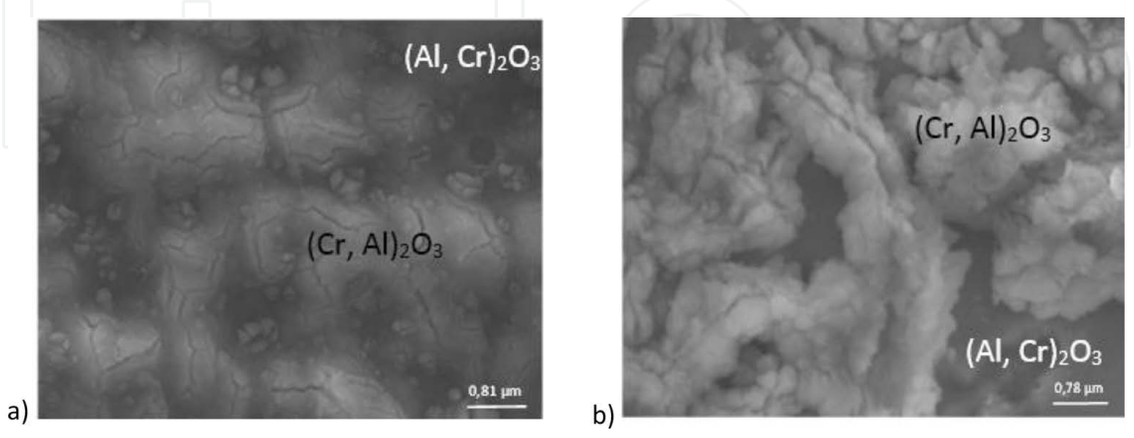

Figure 36. The surface Ti-25Al-12.5Nb-6.01Mo-0.48V coated AlCrN after 100 (a) and 500 (b) hours of isothermal oxidation in air at 800°C.

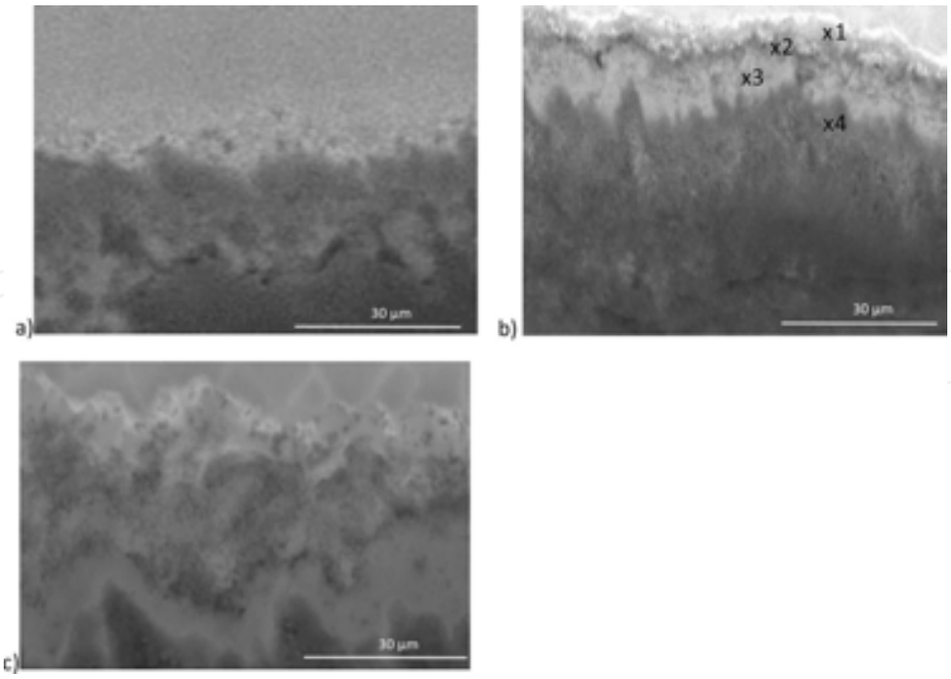

Figure 37. Cross section of the scale formed on Ti-25Al-12.5Nb-6.01Mo-0.48V coated AlCrN after 100 (a); 300 (b) and 500 (c) hours of isothermal oxidation in air at 800°C.

	Al	Ti	Cr	O
×1	20.98	0.96	31.25	46.81
×2	29.21	0.56	21.24	48.99

Table 10. WDS-analysis (at.%) of locations labeled in **Figure 34b**.

	O	Al	Nb	Ti	Cr	N
#1	46.93	20.21	–	1.41	31.45	–
#2	61.57	28.95	–	0.27	9.21	–
#3	–	1.03	1,72	46.47	–	50.78
#4	–	66.21	–	5.78	–	28.01

Table 11. WDS-analysis (at.%) of locations labeled in **Figure 37b**.

As a result of high temperature exposition regardless of the oxidizing environment, the alloy coated with AlCrN forms a scale characterized by lighter and darker contrasting areas (**Figures 34** and **35**). A thin layer rich in chromium-oxide was formed on the surface of the outer layer, while images of cross-section through the formed scale show that the layer of

http://dx.doi.org/10.5772/63998

AlCrN formed during oxidation dissociates, and a two-phase high-porosity oxide mixture takes its place (**Figures 35** and **37**). The chemical composition of specific regions of the scale formed during air oxidation is shown in **Table 10** and on its basis, it may be concluded that darker spots are composed mainly of aluminum oxide with a low quantity of chromium (Item 2), while lighter spots are high-chromium content phase with a lower content of aluminum (Item 1). Observations carried out on cross-section of the scale showed similar chemical compositions (**Table 11**), whereas directly at the interface between the scale and the substrate Ti- and N-rich area is revealed (Item 3) which promotes the formation of titanium nitrides, which depletes the resources of titanium from the metallic substrate at the same time. As a result of the occurring processes, precipitating of Al-rich phase takes place (Item 4). In the case of oxidation at a lower temperature (700°C), similar results were obtained and the dissociation and oxidation of the protective coating was also observed.

Similar results were obtained for the oxidation in the atmosphere containing 9% O_2+ 0.2% HCl + 0.08% SO_2+ N_2. SEM observations showed a scale of homogeneous structure with numerous small discontinuities. During the oxidation in air, the scale composed of the characteristic eruptions forms on the surface, and the scale which is formed during the oxidation in the 9% O_2 + 0.2% HCl + 0.08% SO_2 + N_2 atmosphere is characterized by the presence of needle-shaped oxides growing on its surface and expanding as the oxidation time increases (**Figures 38** and **40**). Compared to the oxidized samples coated with Al_2O_3, the scale is characterized by a compact structure. The cross section of the scale formed in an atmosphere 9% O_2 + 0.2% HCl + 0.08% SO_2 + N_2 shows, similar to the oxidation in the air, the characteristic multi-layered structure with distinct interfaces between the sub-layers (**Figures 39** and **41**). During the oxidation in air, it was observed that the layer closest to the substrate is characterized by irregular structure, with pits inside material and extensive discontinuity propagating between the layers. On the other hand, a thicker layer formed during the oxidation in an aggressive atmosphere has visible and noticeable pores. In this layer, relatively large amount of sulfur and chlorine is also noticeable from the viewpoint of corrosion (**Table 12**).

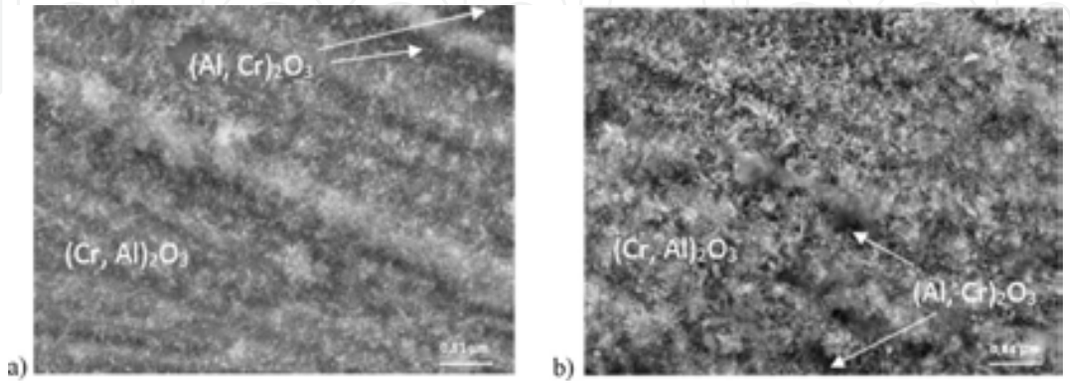

Figure 38. The surface Ti-25Al-12.5Nb-6.01Mo-0.48V coated AlCrN after 100 (a) and 500 (b) hours of isothermal oxidation in 9% O_2+ 0.2% HCl + 0.08% SO_2+ N_2 atmosphere at 700°C.

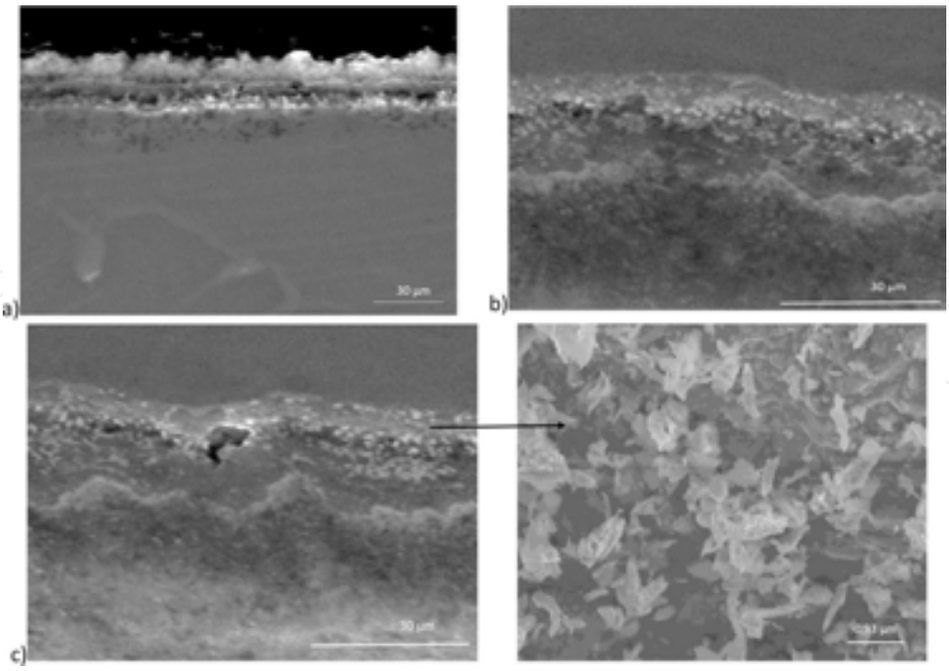

Figure 39. Cross section of the scale formed on Ti-25Al-12.5Nb-6.01Mo-0.48V coated AlCrN after 100 (a); 300 (b) and 500 (c) hours of isothermal oxidation in 9% O_2+ 0.2% HCl + 0.08% SO_2+ N_2 atmosphere at 700°C.

During high-temperature oxidation, AlCrN coating deposited on the test alloy Ti-25Al-12.5Nb-6Mo-0.48V caused the formation of a mixed scale rich in chromium and alumina on the surface, which posed an effective barrier against the diffusion of oxygen. The oxidation of the coated substrate occurs here as a result of in-core diffusion of oxygen and out-core diffusion of coating elements. However, fast out-core diffusion of chromium caused the formation of regions rich in Cr_2O_3 in the outer layer of the scale as well as aluminum rich regions. Despite the fact that due to the impact of high temperature, the AlCrN coating dissociates, and no oxidation of titanium nitride formed under the scale is observed. A completely different process is observed for uncoated specimens where this layer is oxidized to TiO_2 due to the increase of partial pressure and does not provide a sufficient protection.

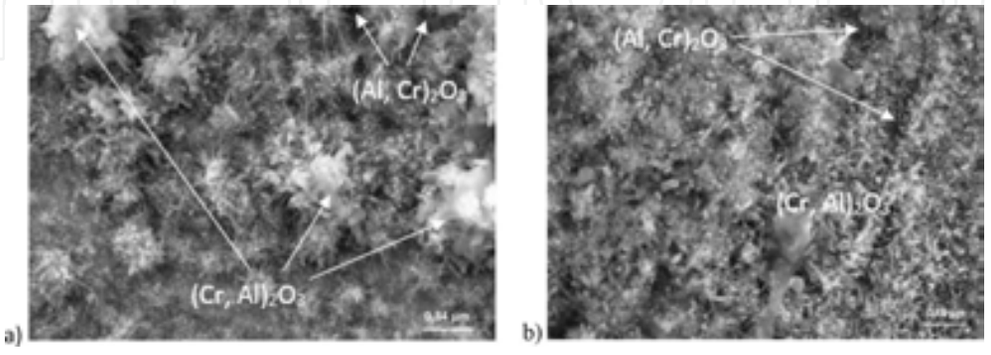

Figure 40. The surface Ti-25Al-12.5Nb-6.01Mo-0.48V coated Al_2O_3 after 100 (a) and 500 (b) hours of isothermal oxidation in 9% O_2+ 0.2% HCl + 0.08% SO_2+ N_2 atmosphere at 750°C.

http://dx.doi.org/10.5772/63998

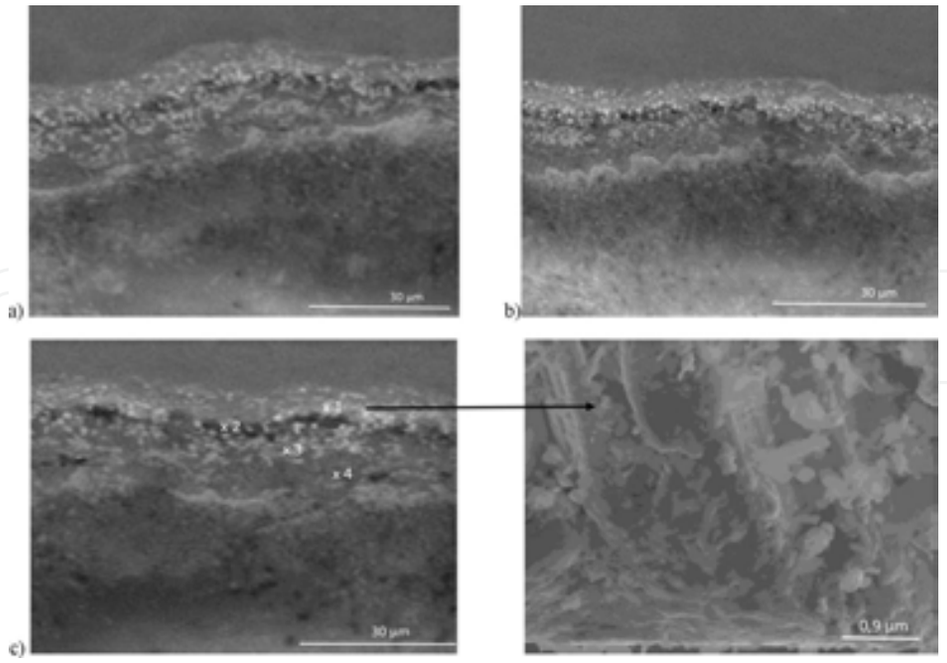

Figure 41. Cross section of the scale formed on Ti-25Al-12.5Nb-6.01Mo-0.48V coated AlCrN after 100 (a); 300 (b) and 500 (c) hours of isothermal oxidation in 9% O_2+ 0.2% HCl + 0.08% SO_2+ N_2 atmosphere at 750°C.

	O	Al	Nb	Ti	Cr	N	S	Cl
#1	44.65	19.97	–	2.17	32.21	–	0.03	0.97
#2	58.88	27.37	–	0.58	10.03	–	0.93	2.21
#3	–	096	2.14	44.87	–	52.03	–	–
#4	–	62.69	–	9.17	–	28.14	–	–

Table 12. WDS-analysis (at.%) of locations labelled in **Figure 41c**.

4. Conclusion

1. During the oxidation of the alloy Ti-25Al-12.5Nb-6.01Mo-0.48V in the initial state in the atmosphere of air a multiphase scale forms, consisting of three layers: an outer layer comprising a mixture of TiO_2 and lower quantity of Al_2O_3, heterogeneous middle layer predominantly composed of Al_2O_3 with small amounts of TiO_2 and an inner layer of comparable quantities of TiO_2 and Al_2O_3.
2. In the case of Ti-25Al-12.5Nb-6.01Mo-0.48V coated with Al_2O_3, during the exposure to high temperature on the surface of the coating layer, reaction products are formed, because a diffusion exchange takes place between the components of the alloy and the protective layer which leads to significant changes in the composition of material and protective layer near the interface coating-substrate. Multiple layered nature of the scale

was proven with delamination and cracks: the scale consists of a thin layer cracked at the material and due to the influence of aggressive atmosphere, its detachment from the substrate material follows. In this case the oxidation of the metallic substrate of O-Ti_2AlN alloy occurred under the coating of Al_2O_3; compact and dense initial Al_2O_3 coating dissolved, and in its place was taken by a porous scale. After partial wear and dissociation of the original Al_2O_3 coating, the in-core diffusion of oxygen and ex-core diffusion of Ti accelerates the scale growth.

3. The surface of the scale formed on the alloy with the coating AlCrN has a definitely different character. The oxidation in the case results in the formation of an oxide scale consisting of a mixture of the two phases of different composition, namely the base phase $(Al, Cr)_2O_3$ and a thin surface layer rich in chromium oxide $(Cr, Al)_2O_3$. Underneath the AlCrN coating, which is subject to partial dissociation, a TiN area is formed along with precipitations of niobium- and aluminum-rich phase.

4. The corrosive process of the alloy Ti-25Al-12.5Nb-6.01Mo-0.48V in the environment of 9% O_2+ 0.2% HCl + 0.08% SO_2+ N_2 is comparable to corrosion occurring in the air; however, in an environment containing even such small quantities of sulfur the material rapidly degrades, which in turn may cause breakaway corrosion. The chemical composition of the scales presented in this paper is similar and its analysis reveals the presence of sulfides and chlorine compounds in the outer layer of the scale, and their share in respective layers is dependent on the temperature and their exposure time.

5. The growth of the multilayered sulfide scales occurs by out-core diffusion of metal cations (Ti, Al, Nb) in the crystallographic lattice structure and in-core diffusion of sulfur and chlorine compounds through discontinuities in the layer surface. The sequence of sublayers and their morphology basically do not differ from the products obtained during oxidation in air because there is practically no difference in the sequence of their formation. A massive difference is, however, the occurrence of distinctive "pits" in respective sublayers, and a specific feature of the scale formed in the aggressive atmosphere is its porous morphology and voids in each sublayer, which definitely promotes the diffusive processes. It can be said that respective sublayers are not compact (as in the case of oxidation in air separated from each other in a characteristic way), which facilitates the transportation of sulfur and chlorine into the material through its discontinuity, and the region closest to the material contains (white band enriched with Nb) oxides limiting the dissolution of sulfur and chlorine.

6. From the very beginning of the test, the role of chlorine in this case is small while the active processes are linked to oxidation and sulfuration. The presence of sulfur at the beginning and the end of the test is the result of discontinuities in the scale, through which occurs the intake of the corrosive atmosphere to naked parts of the material and the resumption of corrosive processes including sulfur. The spallation of the corrosion products does not promote in this case the formation of the oxide layer and initiates the corrosive processes in the naked spots. In consequence, the scale formed in these conditions may reduce the diffusion of chlorine and sulfur, not allowing to form chlorides and sulfides.

Acknowledgements

The research study was financed from the funds for science in 2013–2015 as research project no. IP 2012 055772.

Author details

Joanna Małecka

Address all correspondence to: j.malecka@po.opole.pl

Faculty of Mechanical Engineering, Opole University of Technology, Opole, Poland

References

[1] APPEL F., PAUL J. D. H., OEHRING M.: Gamma titanium aluminide alloys, Wiley-VCH Verlag GmbH (2011).

[2] LORIA A.: Gamma titanium aluminides as prospective structural materials, Intermetallics 8 (2000) 1339–1345.

[3] SZKLINIARZ W.: Metallic materials with the participation of intermetallic phases (in Polish). Z. Bojar and W. Przetakiewicz (Eds.), Technical Military Academy, Warsaw (2006).

[4] KUMPFERT J., LEYENS C.: Titanium and titanium alloys, fundamentals and applications. C. Leyens and M. Peters (Eds.), Wiley-VCH Verlag GmbH & Co. KGaA, Weinheim (2003).

[5] BANERJEE D., GOGIA A. K., NANDY T. K., JOSHI V. A.: A new ordered orthorhombic phase in a Ti_3Al_2Nb alloy, Acta Metallurgica A36 (1988) 871–882.

[6] KUMPFERT J.: Intermetallic alloys based on orthorhombic titanium aluminide, Advanced Engineering Materials 3 (2001) 851–864.

[7] MOZER B., BENDERSKY L. A., BOETTINGER W. J.: Neutron powder diffraction study of the orthorhombic Ti_2AlNb phase, Scripta Metallurgica et Materialia 24 (1990) 2363–2368.

[8] MURALEEDHARAN K., GOGIA A. K., NANDY T. K., BANERJEE D., LELE S.: Transformations in a Ti-24Al-15Nb alloy: part I. Phase equilibria and microstructure, Metallurgical and Materials Transaction A 23A (1992) 401–415.

[9] ROWE R.G., BANERJEE D., MURALEEDHARAN K., LARSEN M., HALL E. L., KONITZER D. G, WOODFIELD A. P.: in Titanium '92 Science and Technology. F. H. Froes and I. Caplan (Eds.) TMS, Warrendale, PA (1993) 1259–1266.

[10] CHAN K. S.: Developing hydrogen-tolerant microstructures for an alpha-2 titanium aluminide alloy, Metallurgical and Materials Transactions 23A (1992) 497–507.

[11] JIQIANG WANG, LINGYAN KONG, TIEFAN LI, TIANYING XIONG: Oxidation behavior of thermal barrier coatings with a $TiAl_3$ bond coat on γ-TiAl alloy, Journal of Thermal Spray Technology 24/3 (2015) 467–475.

[12] KAKARE S.A., TONEY J. B. ASWATH P. B.: Oxidation of ductile particle reinforced Ti-48Al composite, Metallurgical and Materials Transactions 26A (1995) 1835–1845.

[13] TAKASAKI A., FURUYA Y., TANEDA Y.: Hydrogen uptake in titanium aluminides covered with oxide layers, Metallurgical and Materials 29A (1998) 307–314.

[14] YOUNG-WON KIM, WILFRIED SMARSLY, JUNPIN LIN, DENNIS DIMIDUK, FRITZ APPEL (Eds): Gamma Titanium Aluminide Alloys: A collection of research on innovation and commercialization of gamma alloy technology, The Minerals, Metals & Materials Society. Wiley TMS (2014), United States of America.

[15] MROWEC S., WERBER T.: Gas Corrosion of Metals, Publishing House "Silesia" Katowice (1975) (in Polish)

[16] HENCH L., OREFICE R.: Sol–gel technology. Kirk-Othmer Encyclopedia of chemical technology, John Wiley & Sons, Inc. (2000)

[17] BRINKER C. J., SCHERER G. W. (Eds.).: Sol–gel science. The physics and chemistry of sol-gel processing, Gulf Professional Publishing (1990), United States of America

[18] BURAKOWSKI T, WIERZCHOń W.: Surface engineering, WNT, Warszawa 1995 (in Polish).

[19] BACZMARSKI A., BRAHAM C., SEILER W., SHIRAKI N.: Multi-reflecion method and grazing incidence geometry used for stress measurement by X-ray diffraction, Surface and Coatings Technology 182 (2004) 43–54.

[20] KUMPFERT J., ASSLER H., MIRACLE D.B., SPOWART J. E.: Transverse Properties of Titanium Matrix Composites, Proc. of Materials Week 2000, Symposium: Biomimetic Processing of Structural Material, (2000) Munich.

[21] MADER W., RUHLER M.: Electron microscopy studies of defects at diffusion-bonded Nb/Al_2O_3 interface, Acta Mater. 37, 1989, p. 853–866